Differential N-end Rule Degradation of RIN4/NOI Fragments Generated by the AvrRpt2 Effector Protease[1][OPEN]

Kevin Goslin,[a,2,3] Lennart Eschen-Lippold,[b,2] Christin Naumann,[c,e,4] Eric Linster,[e] Maud Sorel,[a] Maria Klecker,[c,d,5] Rémi de Marchi,[a] Anne Kind,[a,6] Markus Wirtz,[e] Justin Lee,[b] Nico Dissmeyer,[c,d,f] and Emmanuelle Graciet[a,7,8]

[a]Department of Biology, Maynooth University, Maynooth, County Kildare, Ireland
[b]Department of Stress and Developmental Biology, Leibniz Institute of Plant Biochemistry, 06120 Halle (Saale), Germany
[c]Independent Junior Research Group on Protein Recognition and Degradation, Leibniz Institute of Plant Biochemistry, 06120 Halle (Saale), Germany
[d]ScienceCampus Halle – Plant-Based Bioeconomy, 06120 Halle (Saale), Germany
[e]Centre for Organismal Studies Heidelberg, Heidelberg University, 69120 Heidelberg, Germany
[f]Institute of Biochemistry and Biotechnology, Martin Luther University of Halle-Wittenberg, 06120 Halle (Saale), Germany

ORCID IDs: 0000-0003-0205-4013 (K.G.); 0000-0001-6972-155X (C.N.); 0000-0002-3586-295X (M.S.); 0000-0001-5508-2363 (M.K.); 0000-0002-8260-8102 (A.K.); 0000-0001-7790-4022 (M.W.); 0000-0001-8269-7494 (J.L.); 0000-0002-4156-3761 (N.D.); 0000-0003-3548-8213 (E.G.).

In plants, the protein RPM1-INTERACTING PROTEIN4 (RIN4) is a central regulator of both pattern-triggered immunity and effector-triggered immunity. RIN4 is targeted by several effectors, including the *Pseudomonas syringae* protease effector AvrRpt2. Cleavage of RIN4 by AvrRpt2 generates potentially unstable RIN4 fragments, whose degradation leads to the activation of the resistance protein RESISTANT TO P. SYRINGAE2. Hence, identifying the determinants of RIN4 degradation is key to understanding RESISTANT TO P. SYRINGAE2–mediated effector-triggered immunity, as well as virulence functions of AvrRpt2. In addition to RIN4, AvrRpt2 cleaves host proteins from the nitrate-induced (NOI) domain family. Although cleavage of NOI domain proteins by AvrRpt2 may contribute to pattern-triggered immunity regulation, the (in)stability of these proteolytic fragments and the determinants regulating their stability remain unexamined. Notably, a common feature of RIN4, and of many NOI domain protein fragments generated by AvrRpt2 cleavage, is the exposure of a new N-terminal residue that is destabilizing according to the N-end rule. Using antibodies raised against endogenous RIN4, we show that the destabilization of AvrRpt2-cleaved RIN4 fragments is independent of the N-end rule pathway (recently renamed the N-degron pathway). By contrast, several NOI domain protein fragments are genuine substrates of the N-degron pathway. The discovery of this set of substrates considerably expands the number of known proteins targeted for degradation by this ubiquitin-dependent pathway in plants. These results advance our current understanding of the role of AvrRpt2 in promoting bacterial virulence.

Plants have evolved complex mechanisms to fight off pathogens. A first line of defense is initiated through the recognition of pathogen-associated molecular patterns by surface-localized transmembrane pattern recognition receptors, resulting in the activation of multiple signal transduction pathways, large transcriptional changes, and the onset of pattern-triggered immunity (PTI; Jones and Dangl, 2006; Henry et al., 2013; Couto and Zipfel, 2016). Pathogens also code for effector proteins or molecules that are secreted. These effectors misregulate different aspects of the PTI response or upstream signaling cascades by hijacking or manipulating the function of host proteins. In the absence of cognate receptors for these effectors, their activity results in dampened host immunity and increased pathogen virulence. However, these effectors may be detected, directly or indirectly, by intracellular nucleotide binding site Leu-rich repeat receptor proteins. This recognition elicits a stronger response, termed effector-triggered immunity (ETI), which is often associated with a localized programmed cell death (Jones and Dangl, 2006; van der Hoorn and Kamoun, 2008; Kourelis and van der Hoorn, 2018).

A key regulator of plant immunity is the membrane-bound protein RPM1-INTERACTING PROTEIN4 (RIN4), which acts as a negative regulator of both PTI and ETI (Day et al., 2005; Kim et al., 2005b; Liu et al., 2009; Afzal et al., 2011; Toruño et al., 2019). Notably, RIN4 is targeted by multiple effector proteins, including AvrRpm1 (Mackey et al., 2002), AvrB (Mackey et al., 2002; Desveaux et al., 2007), HopF2 (Wilton et al., 2010), and HopZ3 (Lee et al., 2015b). The effector protease

AvrRpt2 also targets RIN4 (Axtell et al., 2003; Mackey et al., 2003; Chisholm et al., 2005) as well as other proteins that have the AvrRpt2 consensus recognition sequence PxFGxW (Chisholm et al., 2005; Kim et al., 2005a; Eschen-Lippold et al., 2016a). Following delivery into host cells and plant cyclophilin-dependent activation (Jin et al., 2003; Coaker et al., 2005), AvrRpt2 undergoes autocatalytic cleavage (Axtell et al., 2003; Chisholm et al., 2005) and cleaves RIN4 at two specific sites within the N-terminal or C-terminal nitrate-induced (NOI) domains of RIN4. These are referred to as RIN4 cleavage site 1 (RCS1) and RCS2, respectively (Fig. 1A). In Arabidopsis (*Arabidopsis thaliana*) *rpm1 rps2* double mutant plants lacking functional RESISTANCE TO P. SYRINGAE PV MACULICOLA1 (RPM1) and RESISTANT TO P. SYRINGAE2 (RPS2) nucleotide binding site Leu-rich repeat receptor proteins, these RIN4 fragments suppress PTI (Afzal et al., 2011). RIN4 and its cleavage by AvrRpt2 may also play a role in the regulation of EXOCYST SUBUNIT EXO70 FAMILY PROTEIN B1 (EXO70B1), a subunit of the exocyst complex that is important for autophagic-related protein trafficking (Kulich et al., 2013; Sabol et al., 2017) and plays a role in plant immunity (Stegmann et al., 2013; Liu et al., 2017). Notably, AvrRpt2 also promotes virulence through RIN4-independent mechanisms, including the manipulation of auxin signaling (Chen et al., 2007; Cui et al., 2013) and the repression of mitogen-activated protein kinase pathways (Eschen-Lippold et al., 2016a, 2016b).

In an RPS2 genetic background, cleavage of RIN4 at RCS1 and RCS2 triggers RPS2-mediated ETI (Axtell and Staskawicz, 2003; Mackey et al., 2003; Chisholm et al., 2005; Kim et al., 2005a). The RIN4-II and RIN4-III fragments (Fig. 1A) resulting from cleavage at RCS1 and RCS2, respectively, were shown to be unstable (Axtell et al., 2003; Axtell and Staskawicz, 2003; Mackey et al., 2003), although in some cases, they may be detected for up to 6 h after AvrRpt2 expression or delivery to host cells (Kim et al., 2005a; Afzal et al., 2011). It has nevertheless been proposed that the degradation of these RIN4 fragments could play a role in the activation of RPS2-mediated ETI (Axtell et al., 2003; Axtell and Staskawicz, 2003; Mackey et al., 2003). Experiments with short N-terminal fragments of RIN4 fused to the N terminus of GFP suggested that the ubiquitin-dependent N-end rule pathway, which targets proteins for degradation based on the nature of a protein's N-terminal residue (or N-degron), may play a role in the degradation of the RIN4 fragments (Takemoto and Jones, 2005). However, it is known that recognition of a substrate protein by components of the N-end rule pathway (now renamed the "N-degron pathway" [Varshavsky, 2019]) depends additionally on the conformation of the protein and the accessibility of the N-terminal residue. Hence, an unanswered question is whether the N-degron pathway can indeed target the native RIN4-II and -III fragments for degradation.

While several branches of the N-degron pathways have been uncovered and dissected in yeast and mammals (Varshavsky, 2019), in plants, the so-called Arg/N-degron branch has been the most extensively studied (for review, see Gibbs et al., 2014, 2016; Dissmeyer et al., 2018; Dissmeyer, 2019). When present at the N terminus, so-called primary destabilizing residues of the Arg/N-degron pathway can be recognized by specific E3 ubiquitin ligases, termed N-recognins. In Arabidopsis, at least two N-recognins with different substrate specificities exist, namely, PROTEOLYSIS1 (PRT1) and PRT6 (Potuschak et al., 1998; Stary et al., 2003; Garzón et al., 2007). Other N-terminal residues function as secondary destabilizing residues and require arginylation (i.e. conjugation of Arg, a primary destabilizing residue) by the Arg-transferases ARGININE TRNA PROTEIN TRANSFERASE1 (ATE1) and ATE2 (in Arabidopsis) before they are recognized by PRT6. Last, proteins starting with tertiary destabilizing residues need to be modified before they are arginylated by ATE1/ATE2 and targeted for degradation by PRT6 (Fig. 1B). The plant Arg/N-degron pathway has been shown to regulate various developmental and physiological processes in Arabidopsis (Graciet et al., 2009; Holman et al., 2009; Abbas et al., 2015; Gibbs et al., 2018; Zhang et al., 2018; Weits et al.,

[1]This work was supported by the Science Foundation Ireland (grant no. 13/IA/1870 to E.G.), the Deutsche Forschungsgemeinschaft (DFG) (grant no. LE 2321/3–1 to J.L.), the ScienceCampus Halle – Plant-Based Bioeconomy and DFG (grant no. DI 1794/3–1 to N.D.), a Ph.D. fellowship from the Landesgraduiertenförderung Sachsen-Anhalt (to C.D.), the ERASMUS+ exchange program (to A.K.), and the research in the M.W. group was funded by the DFG via the Collaborative Research Centre (1036 TP 13) and the European Union by the ERA-CAPS (project KatNat).

[2]These authors contributed equally to the article.

[3]Present address: Smurfit Institute of Genetics, Trinity College Dublin, Dublin 2, Ireland

[4]Present address: Department of Molecular Signal Processing, Leibniz Institute of Plant Biochemistry, 06120 Halle (Saale), Germany

[5]Present address: Plant Physiology, University Bayreuth, Universitaetsstr. 30, 95440 Bayreuth, Germany

[6]Present address: Martin-Luther-Universität Halle-Wittenberg, Institut für Pharmazie, Weinbergweg 22, 06120 Halle (Saale), Germany

[7]Author for contact: emmanuelle.graciet@mu.ie.

[8]Senior author.

The author responsible for distribution of materials integral to the findings presented in this article in accordance with the policy described in the Instructions for Authors (www.plantphysiol.org) is: Emmanuelle Graciet (emmanuelle.graciet@mu.ie).

K.G., A.K., and E.G. constructed plasmids used in *Nicotiana benthamiana* and Arabidopsis protoplast experiments, including tFT plasmids; K.G. carried out *N. benthamiana* transient expression experiments, immunoblots, and confocal imaging, as well as all immunoblots for RIN4; L.E.-L. conducted all NOI experiments in Arabidopsis protoplasts, including immunoblots; C.N. and M.K. constructed plasmids for in vitro arginylation assays and performed these assays; E.L. conducted tFT experiments; M.S. and R.d.M. carried out inoculations with *Pst* AvrRpt2 and confocal analysis; E.G., N.D., J.L., and M.W. supervised the experiments; E.G. wrote the article with contributions of all the authors.

[OPEN]Articles can be viewed without a subscription.

www.plantphysiol.org/cgi/doi/10.1104/pp.19.00251

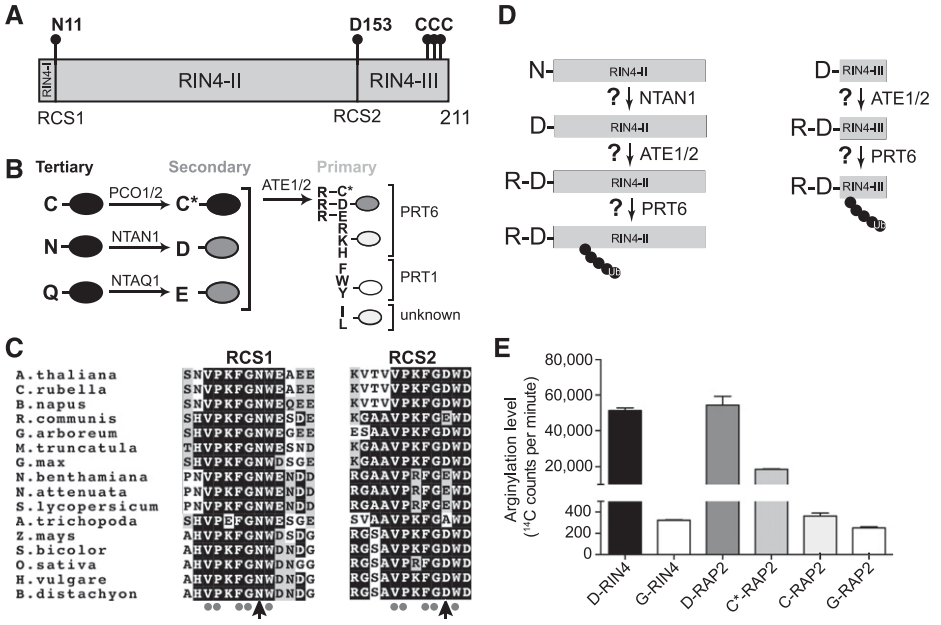

Figure 1. AvrRpt2 cleavage sites and neo-N-terminal residues of RIN4 are conserved and can act as putative N-degron. A, Scheme of AvrRpt2 cleavage sites in Arabidopsis RIN4. RIN4-I, N-terminal fragment of RIN4 released after cleavage at RCS1; RIN4-II, RIN4 fragment following AvrRpt2 cleavage at both RCS1 and RCS2; RIN4-III, C-terminal fragment of RIN4 released after cleavage at RCS2 by AvrRpt2. Newly exposed N-terminal residues (N11 at the N terminus of RIN4-II and D153 at the N terminus of RIN4-III) are indicated. The three C-terminal Cys residues (positions 203 to 205; noted CCC) that are palmitoylated and serve to target RIN4 to the plasma membrane are also indicated. B, Hierarchical organization of the Arg/N-degron pathway in Arabidopsis. Destabilizing N-terminal residues may target proteins for degradation by the ubiquitin-dependent N-degron pathway. Primary destabilizing N-terminal residues are directly recognized by E3 ligases (or N-recognins) of the N-degron pathway, including PRT6 and PRT1. In contrast, secondary destabilizing residues are first modified by Arg-transferases that conjugate Arg at the N terminus of proteins starting with Asp, Glu, and oxidized Cys (noted as Cys*). In addition, tertiary destabilizing residues are first either oxidized by PLANT CYS OXIDASE (PCO) enzymes (in the case of Cys) or deamidated into Asp and Glu by Asn- and Gln-specific deamidases, NTAN1 and NTAQ1, respectively. C, The RCS1 and RCS2 cleavage sites are evolutionarily conserved in plants. Sequence alignment of RCS1 and RCS2 sites from different RIN4 putative orthologs identified using National Center for Biotechnology Information BLASTp with Arabidopsis RIN4 (At3g25070) as a query. Arabidopsis, At3g25070, corresponding to NP_189143.2; *C. rubella*, *Capsella rubella*, XP_023641759.1; *B. napus*, *Brassica napus*, XP_013674753.1; *R. communis*, *Ricinus communis*, XP_002532749.2; *G. arboreum*, *Gossypium arboreum*, KHG28908.1; *M. truncatula*, *Medicago truncatula*, XP_013444158.1; *G. max*, *Glycine max*, NP_001239973.1; *S. lycopersicum*, *Solanum lycopersicum*, XP_010326284.1; *N. benthamiana*, *Nicotiana benthamiana*, APY20266.1; *N. attenuata*, *Nicotiana attenuata*, XP_019249122.1; *A. trichopoda*, *Amborella trichopoda*, XP_011629172.1; *S. bicolor*, *Sorghum bicolor*, XP_002444713.2; *Z. mays*, *Zea mays*, ONM03164.1; *H. vulgare*, *Hordeum vulgare*, AEV12220.1; *B. distachyon*, *Brachypodium distachyon*, XP_003572426.1; *O. sativa*, *Oryza sativa*, BAF24212.1. D, Schematic representation of the different enzymatic modifications required for N-degron–mediated degradation of the RIN4-II and RIN4-III fragments. E, In vitro arginylation of 12-mer peptides derived from the RIN4-II fragment N-terminal region and from known Arg-transferase substrates. RIN4-II peptides with either N-terminal Asp or Gly (noted as D-RIN4-II and G-RIN4-II, respectively; X-WEAEENVPYTA) were synthesized and used in in vitro arginylation assays. Peptides corresponding to the conserved N-terminal sequence of the RAP2.2 and RAP2.12 proteins, which are known Arg-transferase substrates, were also synthesized. Different variants of the latter were used in the in vitro arginylation assays, including peptides with N-terminal Asp, oxidized Cys (denoted as C*), and Gly (peptides noted as D-RAP2, C*-RAP2, and G-RAP2; X-GGAIISDFIPP). Data shown are the average of two independent replicates. Error bars represent standard deviations. C* denotes trioxidized Cys (sulfonic acid, R-SO3H).

2019) and in barley (*Hordeum vulgare*; Mendiondo et al., 2016; Vicente et al., 2017), as well as gametophytic development in the moss *Physcomitrella patens* (Schuessele et al., 2016). Furthermore, protein degradation via this pathway plays a key role in the control of flooding tolerance (Gibbs et al., 2011; Licausi et al., 2011). Importantly, the Arg/N-degron pathway has also been implicated in plant defenses against pathogens (de Marchi et al., 2016; Gravot et al., 2016; Vicente et al., 2019), although a possible connection with AvrRpt2 activity has not been investigated.

In addition to RIN4, AvrRpt2 can cleave other host NOI domain–containing proteins with the AvrRpt2 consensus recognition motifs (Chisholm et al., 2005; Kim et al., 2005a; Takemoto and Jones, 2005; Afzal et al., 2011; Eschen-Lippold et al., 2016a). These NOI proteins have a domain architecture similar to RIN4 (Chisholm et al., 2005; Afzal et al., 2011) and are presumed to be

bound to the plasma membrane (Afzal et al., 2011, 2013). Despite these similarities with RIN4, the role of the NOI domain proteins in either plant immunity or in promoting bacterial virulence following AvrRpt2 cleavage has remained largely elusive. In particular, although many of the NOI domain protein fragments released upon AvrRpt2 cleavage are also predicted to bear destabilizing residues at their N termini (Chisholm et al., 2005), several questions remain unanswered regarding the fate of these fragments: First, are these fragments unstable in host cells following AvrRpt2 cleavage? Second, is N-degron–mediated degradation required to regulate their abundance in planta?

Here, we show that native RIN4 fragments released after AvrRpt2 cleavage are unlikely to be N-degron substrates in a wild-type Arabidopsis background for RPS2. We also show, using selected NOI domain proteins, that the C-terminal fragments released after AvrRpt2 cleavage, which start with a destabilizing residue, are typically unstable. We reveal a role of the N-degron pathway in the degradation of NOI domain proteolytic fragments generated after AvrRpt2 cleavage, so that several of these fragments are genuine N-degron substrates. The latter results open new avenues of research to understand the role of AvrRpt2 in promoting bacterial virulence as well as to dissect the role of the N-degron pathway in the regulation of the plant defense program in response to bacteria encoding the AvrRpt2 protease effector.

RESULTS

A 12-mer RIN4-II N-terminal Peptide Is Arginylated In Vitro

Previously published experiments using a fusion protein composed of the first 30 amino acid residues of RIN4 fused to a C-terminal GFP reporter protein ($RIN4^{1-30}$-GFP) suggested that cleavage of this RIN4 peptide at RCS1 resulted in the N-degron–mediated degradation of the resulting $RIN4^{11-30}$-GFP fusion protein (Takemoto and Jones, 2005). The potential role of the N-degron pathway in clearing these fragments was also strengthened by the overall evolutionary conservation (with some exceptions; Supplemental Fig. S1) of the newly exposed destabilizing N-terminal residue in various RIN4 putative orthologs (Fig. 1C). N-degron–mediated degradation of the $RIN4^{11-30}$-GFP fusion protein, and of the native RIN4-II fragment, would require the deamidation of the newly exposed N-terminal Asn-11 by N-TERMINAL AMIDASE1 (NTAN1) into Asp, followed by arginylation by the Arg-transferases ATE1 and ATE2 (Fig. 1D). Before examining the potential degradation of the native RIN4-II and -III fragments by the N-degron pathway in planta, we first tested if Arabidopsis ATE1 could arginylate the N-terminal sequence of RIN4-II using in vitro arginylation assays in conjunction with 12-mer peptides corresponding to amino acid residues 12–22 of RIN4 preceded by a variable N-terminal residue "X" ($X\text{-}^{12}WEAEENVPYTA^{22}$). The residue X was either an Asp residue (i.e. to mimic the suggested deamidation by NTAN1 of the newly exposed N-terminal Asn-11 into Asp after AvrRpt2 cleavage) or a stabilizing residue, Gly, which is not arginylated. As a control, we generated 12-mer peptides corresponding to the common N-terminal sequence of the RELATED TO AP2.2 (RAP2.2) and RAP2.12 transcription factors, which are known Arg-transferase substrates following dioxygenation of their initial Cys residue (White et al., 2017). In these peptides, amino acid residues 3–13 of the RAP2.2 and RAP2.12 transcription factors were preceded by an N-terminal residue X ($X\text{-}^{3}GGAIISDFIPP^{13}$), which is (1) an oxidized Cys residue or sulfonic acid that can be arginylated; (2) unoxidized Cys (not recognized by Arg-transferases); (3) Asp; or (4) Gly. As hypothesized, based on the known specificity of Arg-transferases in plants (Graciet et al., 2009; Graciet and Wellmer, 2010; White et al., 2017), the RAP2.2 and RAP2.12 peptides starting with oxidized Cys (sulfonic acid) or Asp were arginylated, in contrast to RAP2.2 and RAP2.12 peptides bearing unoxidized thiolated Cys or Gly (Fig. 1E). Importantly, in the same assays, the N-terminal RIN4-II peptide starting with an Asp residue was arginylated in vitro, whereas the same peptide bearing a Gly at the N terminus was not (Fig. 1E). Our in vitro results hence suggest that the N-terminal region of the RIN4-II fragment can serve as an ATE1 substrate in vitro.

AvrRpt2 Cleavage of RIN4 In Planta Results in Unstable Fragments Irrespective of the Presence of a Stabilizing or Destabilizing N-terminal Residue

To address the N-degron–mediated degradation of the native RIN4-II and RIN4-III fragments originating from AvrRpt2 cleavage in planta, we used RIN4-specific antibodies to track the fate of these fragments. We first tested if previously published RIN4-specific antibodies (Mackey et al., 2002; Liu et al., 2009) and a commercially available RIN4 antibody (aN-13, Santa Cruz Biotechnology, catalog no. sc-27369) were suitable to detect full-length RIN4, as well as the RIN4-II and -III fragments. To this aim, we expressed in *Escherichia coli* the RIN4-II and RIN4-III protein fragments, as well as full-length RIN4, as fusion proteins with a poly-His tag and compared the ability of the different RIN4-specific antibodies to recognize these fragments using immunoblotting (Fig. 2A). The results of these experiments indicated that previously published antibodies (designated as anti-RIN4#1 [Mackey et al., 2002] and anti-RIN4#2 [Liu et al., 2009]) were suitable to detect the full-length protein, as well as the RIN4-II and RIN4-III fragments, albeit with different sensitivities. The commercially available anti-RIN4#3 antibody (aN-13) detected both the full-length protein and the RIN4-II fragment, but not the C-terminal RIN4-III fragment, and hence was not suitable for our experiments. All subsequent immunoblots were carried out with the anti-RIN4#2 as the primary antibody.

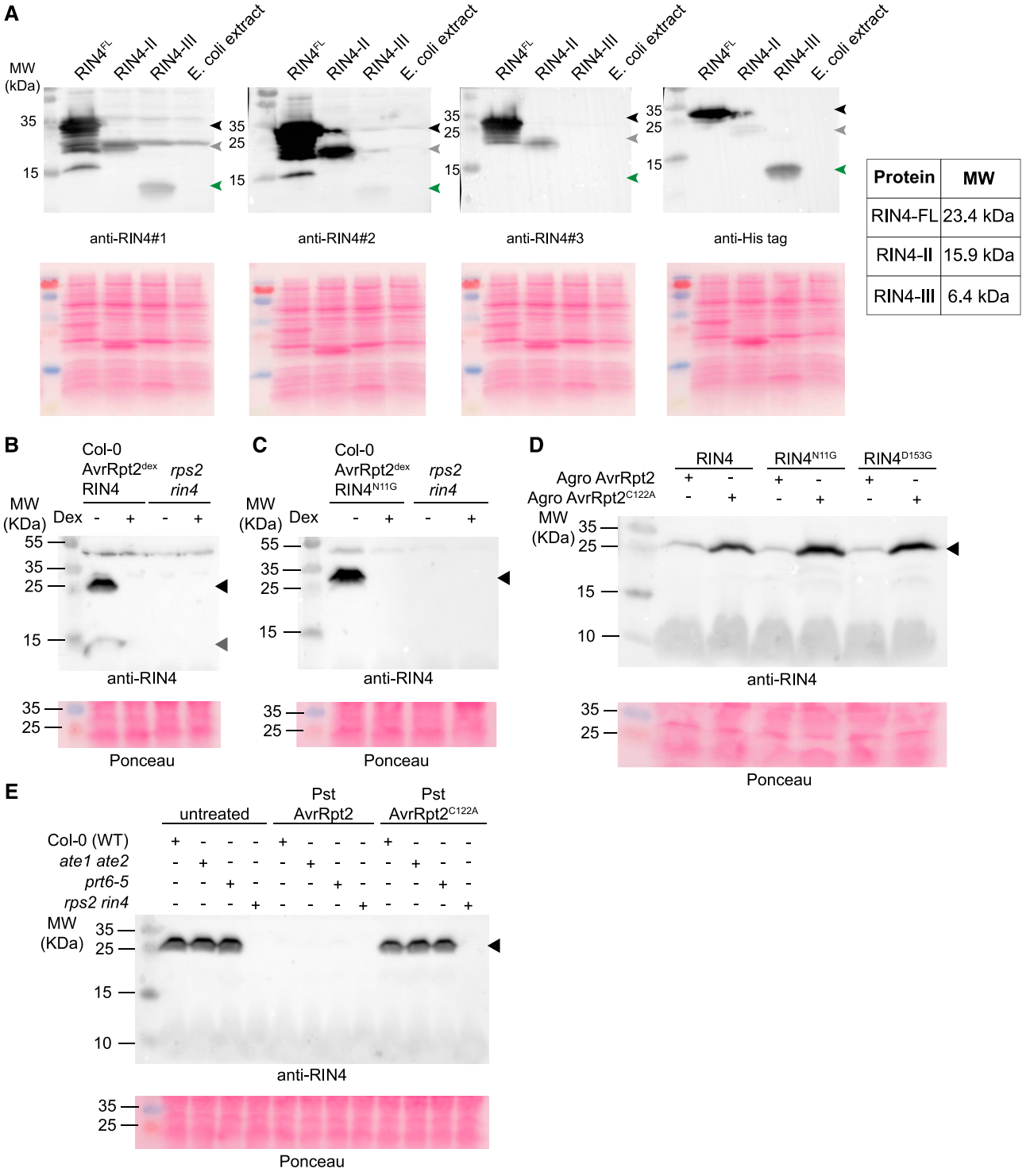

Figure 2. The instability of RIN4-II and RIN4-III proteolytic fragments does not depend on the N-degron pathway. A, Specificity of different antibodies toward RIN4 fragments and the full-length protein. Crude lysates of *E. coli* BL21 Rosetta-GamiB (DE3) expressing 6×His-RIN4 (~27 kD; black arrowhead), 6xHis-RIN4-II (~19.5 kD; gray arrowhead), or 6xHis-RIN4-III (~9.9 kD; green arrowhead) were prepared in 2× Laemmli buffer. The RIN4-specific antibodies used correspond to anti-RIN4#1 (Mackey et al., 2002), anti-RIN4#2 (Liu et al., 2009), and anti-RIN4#3 (aN-13; Santa Cruz Biotechnology). Predicted molecular weights (MW) of untagged full-length RIN4 (RIN4-FL) and proteolytic fragments released following AvrRpt2 cleavage (RIN4-II and RIN4-III). B, Treatment with a dexamethasone-containing solution induces the disappearance of endogenous full-length RIN4 in Col-0 AvrRpt2^{dex} seedlings. Seedlings were grown in liquid 0.5× Murashige and Skoog (MS) medium for 8 d and treated with a dexamethasone-containing solution for 5 h. Black arrowhead indicates full-length RIN4; gray arrowhead indicates a cross-reacting

To investigate the instability of the native RIN4 proteolytic fragments in planta, we conducted immunoblot experiments using protein extracts from wild-type seedlings that also encoded a dexamethasone-inducible version of AvrRpt2 (lines noted Col-0 AvrRpt2^{dex}; Col-0 denoting the accession used). In the absence of dexamethasone (i.e. mock treatment), the endogenous full-length RIN4 protein accumulated in the cells (Fig. 2B; Supplemental Fig. S2). In these conditions, a protein fragment of ~12 kD was also detected by the anti-RIN4#2 antibody. However, longer exposure of the same immunoblot indicated that this protein was also detected in *rps2 rin4* double mutant plants (Supplemental Fig. S2), suggesting that it corresponds to a nonspecific cross-reacting protein. When expression of AvrRpt2 was induced by dexamethasone treatment for 5 h, the full-length RIN4 protein was no longer detectable, as a result of its cleavage by AvrRpt2. In addition, the RIN4-II and RIN4-III fragments could not be detected, suggesting that the two proteolytic fragments were unstable (Fig. 2B; Supplemental Fig. S2). We next tested the importance of the newly exposed destabilizing residue (Asn-11) of the RIN4-II fragment for degradation. To this aim, we generated stable Arabidopsis Col-0 AvrRpt2^{dex} lines that also expressed the full-length RIN4 in which Asn-11 was substituted to Gly (RIN4^{N11G}) under the control of the constitutive *Cauliflower mosaic virus* 35S promoter (lines designated as AvrRpt2^{dex} RIN4^{N11G}). This mutation was unlikely to affect cleavage of RIN4 by AvrRpt2 because AvrRpt2 recognizes motifs with a Gly residue at the same location (Chisholm et al., 2005). While full-length RIN4^{N11G} accumulated in the absence of dexamethasone, the induction of AvrRpt2 expression led to a loss of full-length RIN4^{N11G}, but not to the accumulation of the RIN4-II^{N11G} proteolytic fragment. The absence of RIN4-II^{N11G} detection suggests that the presence of an N-terminal stabilizing residue, such as Gly, failed to stabilize the RIN4-II fragment in planta (Fig. 2C).

To verify these results, we also conducted transient expression experiments in *N. benthamiana* using coinfiltration with *A. tumefaciens* strains encoding AvrRpt2 or AvrRpt2^{C122A} (a catalytically inactive AvrRpt2 [Axtell et al., 2003]) and *A. tumefaciens* strains coding for different versions of the full-length RIN4 protein, including a wild-type version of the protein, an RIN4^{N11G} mutant, or an RIN4^{D153G} mutant, which contains an Asp-153 to Gly substitution at the N terminus of the RIN4-III fragment generated by AvrRpt2 cleavage. Immunoblot analysis using tissue collected 24 h after coinfiltration indicated that expression of neither RIN4^{N11G} nor RIN4^{D153G} impaired cleavage by AvrRpt2, as the full-length version of the protein decreased in abundance similarly to the wild type (Fig. 2D; Supplemental Fig. S2). Furthermore, accumulation of RIN4-II^{N11G} and RIN4-III^{D153G} fragments was not observed, suggesting that in planta destabilization of the full-length, untagged RIN4-II and RIN4-III fragments released after AvrRpt2 cleavage does not require the presence of an N-terminal destabilizing residue.

AvrRpt2 Cleavage of RIN4 In Planta Results in Unstable Fragments in Arabidopsis N-degron Pathway Mutant Backgrounds

To further test the potential N-degron–mediated degradation of both the RIN4-II and -III fragments in planta with the least possible disruption to their conformation and expression levels, we assessed the stability of the native fragments released from endogenous RIN4 in wild-type and mutant backgrounds for the Arg-transferases (*ate1 ate2* mutant; Graciet et al., 2009; Holman et al., 2009) and for the N-recognin PRT6 (*prt6-5*; Graciet et al., 2009). If the RIN4-II and -III fragments are indeed N-degron pathway substrates, we would predict them to be stabilized in the *ate1 ate2* and *prt6-5* mutants (Fig. 1D) after inoculation with a *Pseudomonas syringae* pv tomato DC3000 (*Pst*) strain expressing AvrRpt2. As a control experiment for potential effects by other *Pst* (effector) proteins, we also inoculated the wild-type and mutant plants with a *Pst* strain containing the inactive AvrRpt2^{C122A} variant (Fig. 2E; Supplemental Fig. S2). Immunoblot analysis of the protein extracts indicates that inoculation with *Pst* AvrRpt2, but not with *Pst* AvrRpt2^{C122A}, results in disappearance of the full-length endogenous RIN4 protein as a result of AvrRpt2 activity at 8 hours postinoculation (hpi). However, neither the RIN4-II nor the

Figure 2. (*Continued.*)
protein, which is also detected in *rin4 rps2* samples with longer exposure times (Supplemental Fig. S2). Data shown are representative of three independent replicates. C, Induction of AvrRpt2 expression also triggers the disappearance of full-length RIN4^{N11G} in Col-0 AvrRpt2^{dex} 35S$_{pro}$: RIN4^{N11G} seedlings. The Gly–RIN4-II fragment is not detected despite the presence of a stabilizing N- terminal residue. Seedlings were grown in liquid 0.5× MS medium for 8 d and treated with a dexamethasone-containing solution for 5 h. Arrowhead indicates full-length RIN4. Data are representative of three independent replicates. D, ^{N11G}RIN4-II and ^{D153G}RIN4-III fragments are not stabilized in *N. benthamiana*. Four-week-old *N. benthamiana* plants were coinfiltrated with *Agrobacterium tumefaciens* strains coding for different versions of RIN4 and either an active or inactive variant of AvrRpt2. Tissue for immunoblot was collected 24 h after coinfiltration. Arrowhead indicates full-length RIN4. Data are representative of two independent replicates. E, RIN4-II and -III fragments are not stabilized in mutant backgrounds for N-degron pathway enzymatic components. Plants of the indicated genotypes were left untreated or were inoculated with *Pst* AvrRpt2 or *Pst* AvrRpt2^{C122A} (5×10^7 colony forming units/mL). Inoculated leaves were collected at 8 hpi for immunoblot analysis with the anti-RIN4#2 antibody. Arrowhead indicates full-length RIN4. Data are representative of three independent replicates. For all panels, original data are presented in Supplemental Figure S2.

RIN4-III fragments accumulated in the two mutant backgrounds.

Taken together, our data suggest that, in planta, destabilization of the RIN4-II and -III fragments released after AvrRpt2 cleavage does not require the N-degron pathway.

The Relative Lifetime of the RIN4-II and RIN4-III Fragments Is Similar in *ate1 ate2* and Wild-Type Plants

The experiments conducted above allowed us to monitor the accumulation of the RIN4-II and -III fragments within a few hours after RIN4 cleavage by AvrRpt2. Although a genuine N-degron substrate should be stabilized in these conditions, the experimental approaches did not allow us to compare the degradation rate of the different fragments. To obtain a more accurate estimate of the relative lifetime of the RIN4-II and -III fragments in planta, we used the tandem fluorescent timers technique (tFT; Khmelinskii et al., 2012, 2016), which has recently been developed for plant-based systems (Zhang et al., 2019). In this approach, a protein may be expressed as a fusion consisting of ubiquitin, followed by a residue X; the sequence of the protein/fragment of interest; mCherry; and finally, superfolder GFP (sfGFP). In these fusion proteins, the N-terminal ubiquitin moiety is cleaved off by deubiquitylating enzymes after the last residue of ubiquitin (Varshavsky, 2005), thus resulting in a X-protein-mCherry-sfGFP (X-protein-tFT) fusion protein with the residue X at the N terminus. Measuring the ratio of the slow maturing mCherry to fast maturing sfGFP fluorescence intensities allows the study, in a more dynamic manner, of the relative lifetime of the

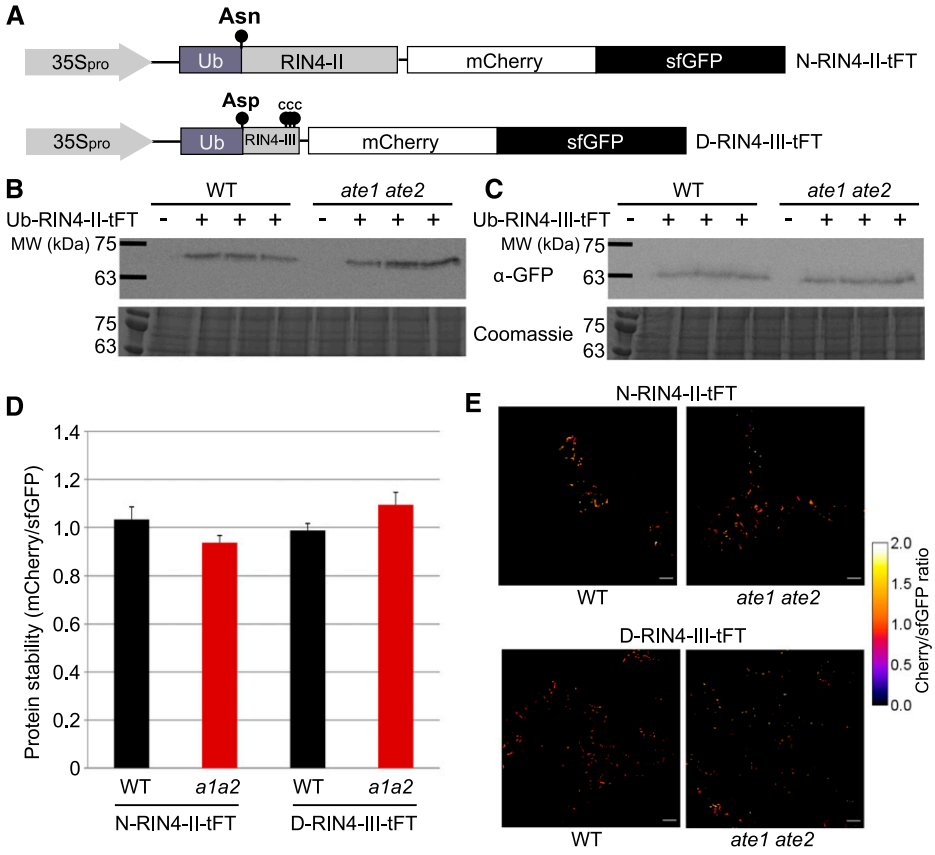

Figure 3. The relative lifetime of RIN4-II-tFT and RIN4-III-tFT fusion proteins is similar in wild-type (WT) and *ate1 ate2* plants. A, Schematic representation of the ubiquitin fusion tFT constructs generated to determine the relative lifetime of the RIN4-II and -III fragments. The N-terminal residues exposed after cleavage of ubiquitin are indicated (i.e. Asn for RIN4-II and Asp for RIN4-III). B, Immunoblot analysis of the RIN4-II-tFT fusion protein. C, Immunoblot analysis of the RIN4-III-tFT fusion protein. For (B) and (C), leaf tissue was collected 4 d after transformation of 5-week-old wild type or *ate1 ate2* mutant plants. Each sample consisted of a pool from six transformed plants. A GFP-specific antibody was used to detect the tFT fusion protein. Original, uncropped data are presented in Supplemental Figure S3. D, Protein stability of the RIN4-II-tFT and RIN4-III-tFT fusion proteins in epidermal cells of 5-week-old wild type or *ate1 ate2* (*a1a2*) mutant plants, as determined by the ratio of mCherry to sfGFP fluorescence intensity. Values represent the mean and SE of five to seven independent replicates and are not significantly different (one-way ANOVA, ANOVA). E, Representative false-color images of Arabidopsis leaf epidermal cells expressing RIN4-II-tFT and RIN4-III-tFT reporters for calculation of mCherry to sfGFP ratios. The heatmap indicates the intensity ratio of mCherry to sfGFP, with blue corresponding to an unstable protein and white a stable one. Scale bars = 50 μm.

fusion protein. Importantly, this technique has been validated in Arabidopsis using the N-degron tFT reporter constructs ubiquitin-Met-tFT (Ub-M-tFT) and Ub-R-tFT in the wild type and in a *prt6-5* mutant background (Zhang et al., 2019), showing that it is suitable to study N-degron–mediated degradation.

To apply the tFT approach, we generated constructs similar to those used by Zhang et al. (2019), which allowed the expression of Ub-N-RIN4-II-tFT or Ub-D-RIN4-III-tFT fusions (Fig. 3A) under the control of the 35S promoter. Immunoblot analysis with a GFP-specific antibody confirmed that the Ub-N-RIN4-II-tFT or Ub-D-RIN4-III-tFT fusions were deubiquitylated and expressed at sufficient levels following transient expression in Arabidopsis leaves (Fig. 3, B and C; Supplemental Fig. S3). Hence, we used confocal imaging to determine the ratio of mCherry/sfGFP fluorescence. Our results indicate that the relative stability of the resulting N-RIN4-II-tFT and D-RIN4-III-tFT proteins was not significantly different in wild-type and *ate1 ate2* mutant backgrounds (Fig. 3D). These results further suggest that the RIN4-II and -III fragments are not N-degron pathway substrates. However, N-RIN4-II-tFT and D-RIN4-III-tFT did not exhibit the expected cytosolic and plasma membrane localization (Fig. 3E; Supplemental Figs. S4 and S5), respectively (Kim et al., 2005a; Takemoto and Jones, 2005; Afzal et al., 2011), which may have impaired their potential N-degron–mediated degradation (see also "Discussion").

A Subset of NOI C-terminal Proteolytic Fragments Are Unstable and Accumulate upon Mutation of the Newly Exposed N-terminal Destabilizing Residue

In addition to RIN4, AvrRpt2 has been shown to cleave other host NOI domain–containing proteins (Chisholm et al., 2005; Takemoto and Jones, 2005; Afzal et al., 2011; Eschen-Lippold et al., 2016a). AvrRpt2 cleavage of several NOI proteins is also predicted to generate proteolytic fragments starting with secondary destabilizing residues (Table 1), which could be sufficient to target them for degradation by the N-degron pathway, following arginylation and recognition by PRT6. To test the potential N-degron–dependent degradation of these C-terminal fragments, we selected for our analysis six different NOI proteins among the 14 NOI domain proteins predicted to be encoded in the Arabidopsis genome. NOI1, NOI2, NOI3, NOI5, NOI6, and NOI11 were chosen to cover members of different clades (Eschen-Lippold et al., 2016a). NOI5, which is the closest in sequence to NOI1, was also included to test if closely related NOIs behave similarly. Next, we designed double-tagged versions of the six NOI proteins (Fig. 4A) to allow their expression as double-tagged proteins with GFP and a hemagglutinin (HA) tag (protein fusion noted GFP-NOI-HA) under the control of the 35S promoter.

We first determined the subcellular localization of the double-tagged NOI proteins to check their predicted plasma membrane localization using transient expression in *N. benthamiana* epidermal cells. A control GFP-luciferase fusion protein localized in the cytoplasm of *N. benthamiana* epidermal cells (Fig. 4, B and C). In contrast, all GFP-NOI-HA proteins localized mostly to the periphery of epidermal cells (Fig. 4, untreated), in agreement with their predicted subcellular localization (Afzal et al., 2013). The GFP-NOI2-HA fusion protein also displayed a strong nuclear signal (Fig. 4, F and G). Epidermal peels were additionally used for closer inspection of the localization, where overlay of chlorophyll autofluorescence and GFP fluorescence revealed GFP-NOI2-HA signals surrounding the chloroplasts (Supplemental Fig. S6). In addition, the GFP-NOI6-HA

Table 1. *Several NOI proteolytic fragments generated after AvrRpt2 cleavage are potential N-degron substrates*

Proteolytic fragments predicted to be released after AvrRpt2 cleavage of several NOI proteins (Chisholm et al., 2005) start with N-terminal destabilizing residues. All fragments would require the activity of the Arg-transferases and PRT6 for N-degron–mediated degradation. The corresponding gene numbers (Arabidopsis Genome Initiative [AGI]) and predicted newly exposed N-terminal residues after AvrRpt2 cleavage are indicated.

AGI	Protein Name	Predicted N-terminal Residue of AvrRpt2 Cleavage Product
At3g25070	RIN4-II fragment	Asn (N)
At3g25070	RIN4-III fragment	Asp (D)
At5g64850	NOI6	Asp (D)
At5g09960	NOI7	Asp (D)
At5g48657	NOI10[a]	Asp (D)
At3g07195	NOI11	Asp (D)
At5g63270	NOI1	Glu (E)
At5g40645	NOI2	Glu (E)
At2g17660	NOI3	Glu (E)
At5g55850	NOI4	Glu (E)
At3g48450	NOI5	Glu (E)
At5g18310	NOI8	Glu (E)

[a]The representative protein model of NOI10 (At5g48657.1) is not cleaved by AvrRpt2 because of a lack of the conserved cleavage site (Eschen-Lippold et al., 2016a).

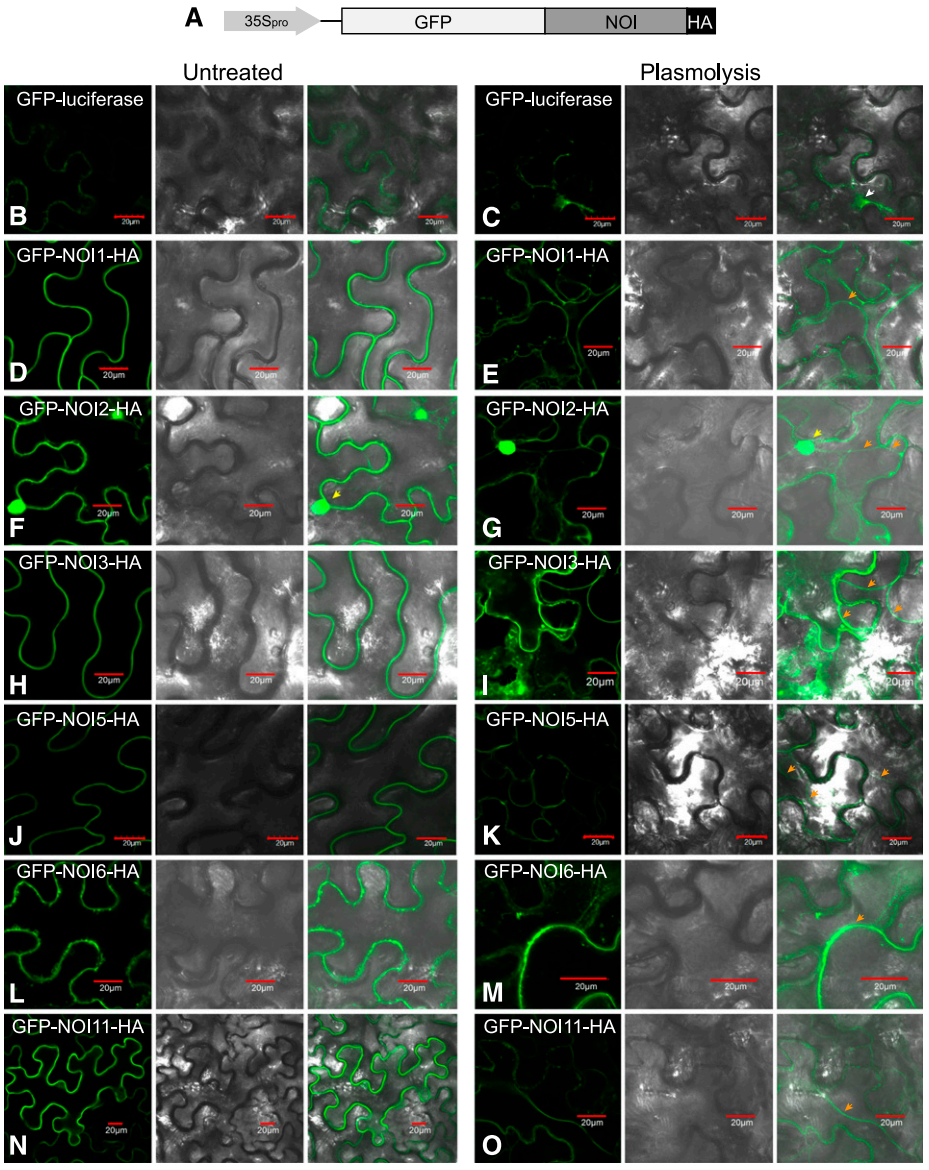

Figure 4. Subcellular localization of GFP-NOI-HA proteins. A, Schematic representation of the double-tagged GFP-NOI-HA constructs under the control of the 35S promoter. B to O, Confocal microscopy images of epidermal cells from *N. benthamiana* leaves (abaxial side) 3 d after infiltration with *A. tumefaciens* coding for the different GFP-NOI-HA constructs. "Untreated" leaf sections (left) were imaged in water. To verify the plasma membrane localization, the same leaf sections were imaged in a 1 M NaCl solution ("plasmolysis"; right). White arrow indicates cytosolic localization of the GFP-luciferase fusion protein following plasmolysis; orange arrows indicate plasma membrane localization; yellow arrows point to nuclear localization. Scale bars = 20 μm.

fusion protein appeared to localize in small intracellular vesicle-like structures (Fig. 4L; Supplemental Fig. S6), which could be in agreement with its interaction with the exocyst complex subunits EXO70A1 and EXO70B1 (Afzal et al., 2013; Sabol et al., 2017). Confocal imaging of the same fusion proteins following plasmolysis further confirmed that the different GFP-NOI-HA proteins are plasma membrane located (Fig. 4, plasmolysis), with GFP-NOI3-HA possibly also localizing to the cytoplasm following plasmolysis (Fig. 4I). In summary, the GFP-NOI-HA–tagged proteins appear to localize as predicted based on their sequence and known protein interactors, suggesting that the double GFP/HA tags are unlikely to affect their subcellular localization.

We next tested if the GFP-NOI-HA fusion proteins were cleaved by AvrRpt2, and whether the C-terminal $^{\Delta}$NOI-HA fragments released after AvrRpt2 cleavage were unstable (Fig. 5; Supplemental Fig. S7). To this aim, we infiltrated 4-week-old *N. benthamiana* plants with different *A. tumefaciens* strains carrying a transfer DNA coding for each of the GFP-NOI-HA constructs. After 72 h, the same leaves were infiltrated with either *Pst* AvrRpt2 or *Pst* AvrRpt2^{C122A}. *Pst* infiltration was carried out 72 h after agroinfiltration to allow for sufficient accumulation of the GFP-NOI-HA fusion proteins, and tissue was collected 10 h after *Pst* inoculation. For each construct, immunoblots were performed with an anti-GFP and an anti-HA antibody to (1) verify the cleavage of the GFP-NOI-HA fusion proteins and (2) test the stability of the N-terminal GFP-NOI$^{\Delta}$ and C-terminal $^{\Delta}$NOI-HA fragments (Fig. 5C). Coexpression of the GFP-NOI-HA constructs and active AvrRpt2 resulted in the cleavage of all GFP-NOI-HA fusion proteins tested, as indicated by the disappearance of full-length fusion proteins concomitantly with the detection of an N-terminal GFP-NOI$^{\Delta}$ fragment in the presence of *Pst* AvrRpt2, but not *Pst* AvrRpt2^{C122A}. Notably, the C-terminal $^{\Delta}$NOI-HA fragments were not

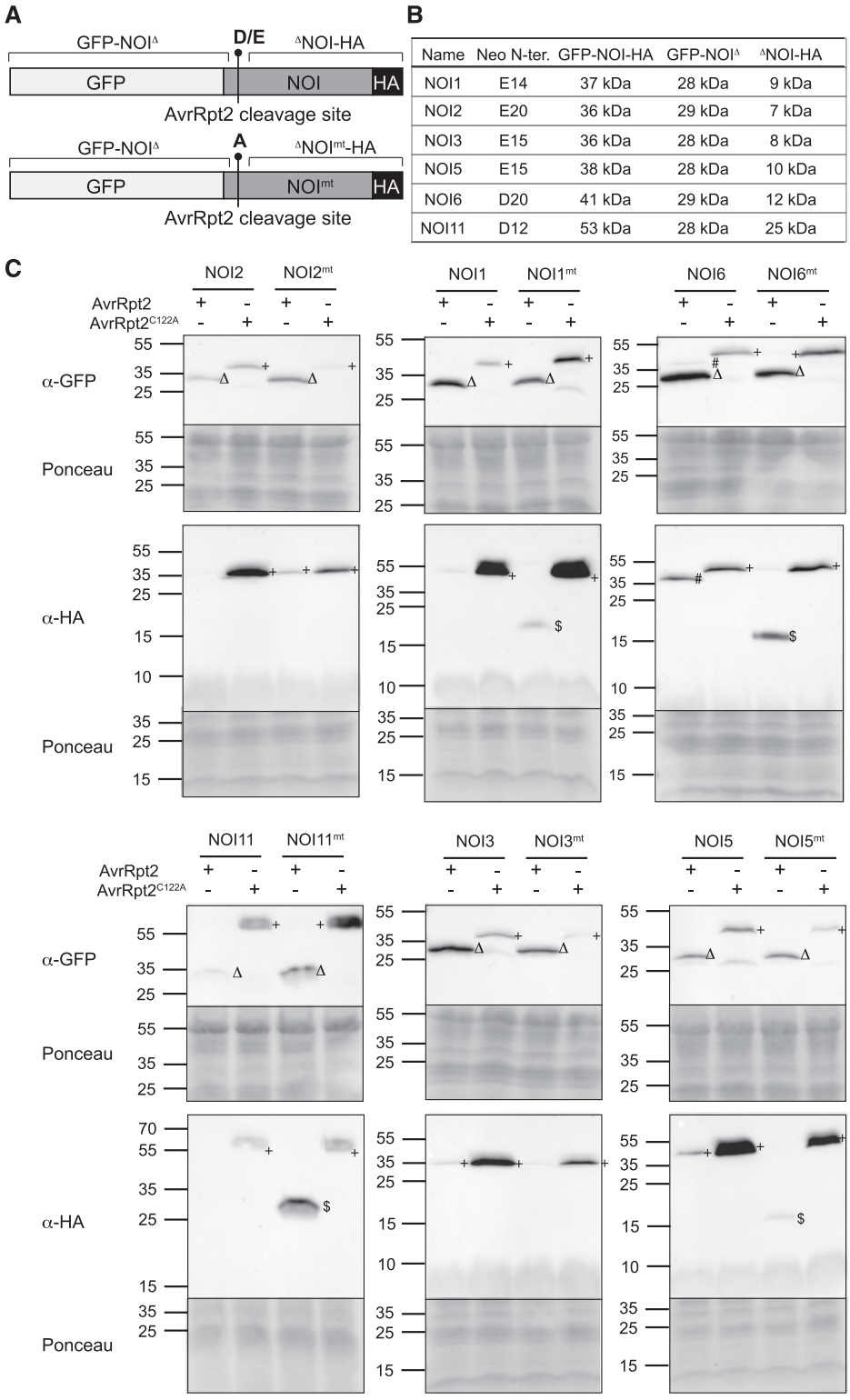

Name	Neo N-ter.	GFP-NOI-HA	GFP-NOIΔ	ΔNOI-HA
NOI1	E14	37 kDa	28 kDa	9 kDa
NOI2	E20	36 kDa	29 kDa	7 kDa
NOI3	E15	36 kDa	28 kDa	8 kDa
NOI5	E15	38 kDa	28 kDa	10 kDa
NOI6	D20	41 kDa	29 kDa	12 kDa
NOI11	D12	53 kDa	28 kDa	25 kDa

Figure 5. Stability of ΔNOI-HA and ΔNOImt-HA fragments in *N. benthamiana*. A, Schematic representation of the GFP-NOI-HA and GFP-NOImt-HA constructs. The predicted AvrRpt2 cleavage site is indicated, as well as the newly exposed Asp or Glu N-terminal residues (destabilizing residues [D/E]) for wild-type sequences, or Ala (stabilizing residue) for the mutated version of the constructs (noted as mt). GFP-NOIΔ refers to the N-terminally GFP-tagged fragments obtained after AvrRpt2 cleavage; ΔNOI-HA and ΔNOImt-HA correspond to the C-terminal HA-tagged NOI fragments released after AvrRpt2 cleavage of the wild-type or mutated NOI proteins, respectively. B, List of NOI proteins for which double-tag GFP-NOI-HA constructs were generated. The nature and position of the newly exposed N-terminal residue after AvrRpt2 cleavage is indicated (Neo N-ter.), as well as the calculated molecular weight of the different full-length fusion proteins and proteolytic fragments. C, Stability of the GFP-NOIΔ, ΔNOI-HA, and ΔNOImt-HA fragments. *N. benthamiana* plants transiently expressing the GFP-NOI-HA or GFP-NOImt-HA fusion proteins from the 35S promoter were inoculated with *Pst* AvrRpt2 or *Pst* AvrRpt2C122A. N-terminal fragments were detected using antibodies directed against the GFP tag (α-GFP), while C-terminal fragments were detected using anti-HA antibodies (α-HA). +, Full-length GFP-NOI-HA–tagged proteins; Δ, GFP-NOIΔ fragments; $, ΔNOImt-HA fragments; #, aspecific cleavage product of GFP-NOI6-HA. These experiments were conducted three times independently with similar results. For all panels, original data are presented in Supplemental Figure S7. Note that the apparently higher molecular weight of the ΔNOI1mt-HA fragment is caused by a distortion in the migration pattern on the gel (Supplemental Fig. S7).

detected using an anti-HA antibody, demonstrating that these fragments are unstable in *N. benthamiana* (Fig. 5C; Supplemental Fig. S7).

Because the ΔNOI-HA fragments are predicted to start with a destabilizing residue, we tested a potential role of the N-degron pathway in their degradation by generating GFP-NOImt-HA constructs, in which the newly exposed N-terminal destabilizing residue was changed into a stabilizing Ala residue (see Fig. 5B for specific mutations introduced in each of the NOI proteins). We then compared the accumulation of the ΔNOI-HA and ΔNOImt-HA fragments. AvrRpt2 cleavage

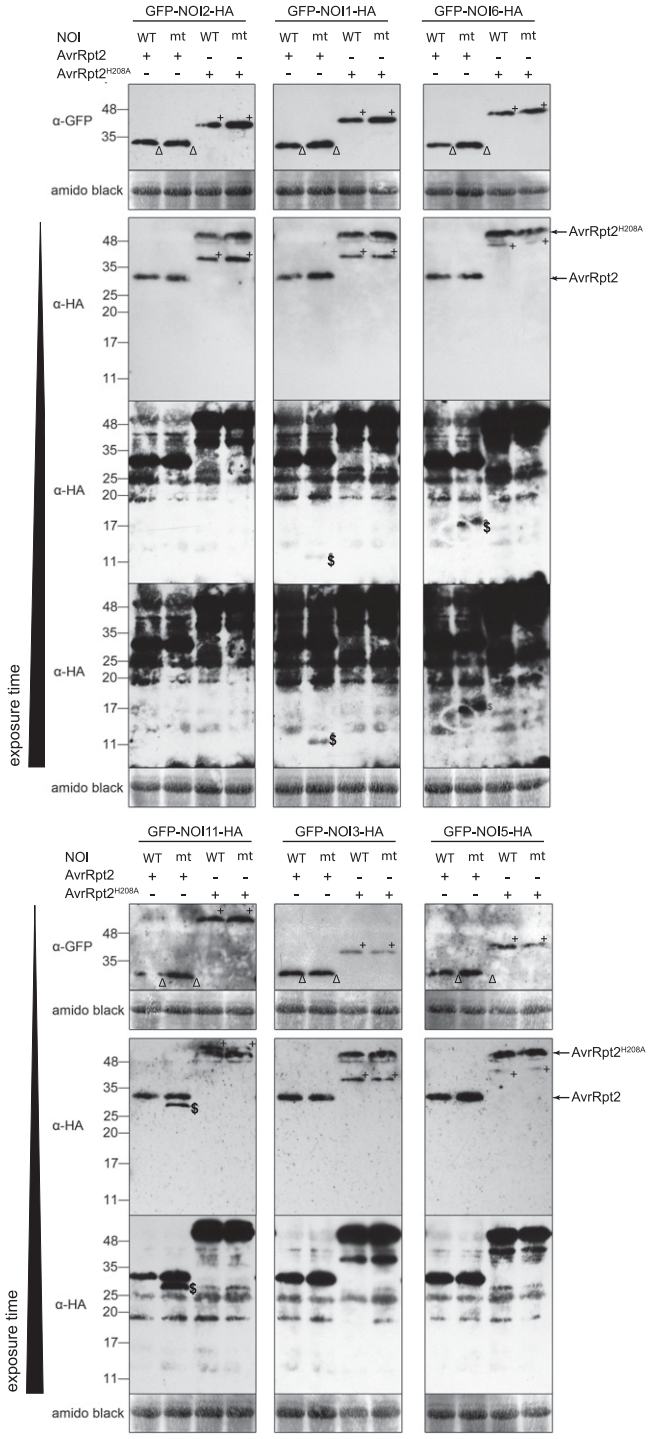

Figure 6. Stability of $^{\Delta}$NOI-HA and $^{\Delta}$NOI^{mt}-HA fragments in wild-type (WT) Arabidopsis protoplasts. Stability of the GFP-NOI$^{\Delta}$, $^{\Delta}$NOI-HA, and $^{\Delta}$NOI^{mt}-HA fragments upon transient coexpression of GFP-NOI-HA and either wild-type AvrRpt2-HA or the AvrRpt2^{H208A}-HA inactive variant. N-terminal fragments were detected using antibodies directed against the GFP tag (α-GFP), while C-terminal fragments were detected using anti-HA antibodies (α-HA). For immunoblots with the anti-HA antibody, images of the same membrane with increasing exposure times are presented to show more clearly the stabilization of the different $^{\Delta}$NOI^{mt}-HA fragments. +, Full-length GFP-NOI-HA–tagged proteins; Δ, GFP-NOI$^{\Delta}$ fragments; $, $^{\Delta}$NOI^{mt}-HA fragments; arrows indicate the self-processed AvrRpt2, as well as the unprocessed inactive AvrRpt2^{H208A} protease. Note that AvrRpt2^{H208A} was expressed from a split-yellow fluorescent protein construct carrying an additional C-terminal yellow fluorescent protein tag at the C terminus. For all panels, original data are presented in Supplemental Figure S8. Data are representative of three independent replicates.

of GFP-NOI^{mt}-HA fusion proteins was overall unaffected by the mutation introduced. Notably, the AvrRpt2-mediated cleavage of four GFP-NOI^{mt}-HA proteins—specifically, NOI1, NOI5, NOI6, and NOI11—generated detectable levels of the respective $^{\Delta}$NOI^{mt}-HA fragments in *N. benthamiana* 10 h after *Pst* AvrRpt2 inoculation. This result suggests that NOI1, NOI5, NOI6, and NOI11, but not NOI2 and NOI3, could be potential N-degron pathway substrates.

To rule out any possible effects of other *Pst* DC3000 effector proteins on the processing and stability of the $^{\Delta}$NOI-HA fragments, we conducted transient expression experiments in wild-type Arabidopsis protoplasts that were cotransfected with constructs coding for (1) wild-type AvrRpt2 or the inactive AvrRpt2^{H208A} variant (Cui et al., 2013), and (2) the double-tagged GFP-NOI-HA or GFP-NOI^{mt}-HA proteins. Proteins were then extracted for immunoblotting with anti-GFP and anti-HA antibodies. Similar to the results obtained in *N. benthamiana*, coexpression of wild-type AvrRpt2 with either GFP-NOI-HA or GFP-NOI^{mt}-HA resulted in cleavage of the fusion proteins (Fig. 6; Supplemental Fig. S8). Furthermore, the $^{\Delta}$NOI-HA fragments released after cleavage of the wild-type double-tagged NOI proteins could not be detected in immunoblots with an anti-HA antibody, even after long exposure times (Fig. 6). In contrast, $^{\Delta}$NOI^{mt}-HA fragments accumulated to detectable levels with NOI1, NOI6, and NOI11, but not for NOI2, NOI3, and NOI5 (Fig. 6). Hence, irrespective of whether the AvrRpt2 effector was delivered via *Pst* or by direct AvrRpt2 expression in plant cells, our data suggest that the $^{\Delta}$NOI^{mt}-HA fragments obtained after cleavage of NOI1, NOI6, and NOI11could be N-degron pathway substrates. In contrast, fragments obtained after cleavage of NOI2, NOI3, and NOI5 are not substrates in Arabidopsis.

Specific $^{\Delta}$NOI-HA Protein Fragments Constitute N-degron Pathway Substrates In Planta

To further verify the N-degron–dependent degradation of the $^{\Delta}$NOI-HA fragments, we conducted cotransfection experiments in protoplasts derived from wild-type (Col-0) plants, as well as from the *ate1 ate2* and *prt6-1* (Garzón et al., 2007) mutants, which are affected for Arg-transferases and PRT6 (Fig. 1A). The use of these mutant plants in conjunction with the GFP-NOI-HA constructs allowed us to rule out possible non-N-degron–dependent effects of the mutation introduced in the GFP-NOI^{mt}-HA constructs on the stability of the resulting fragments after AvrRpt2 cleavage. Coexpression of either GFP-NOI2-HA or GFP-NOI5-HA

with AvrRpt2 in *ate1 ate2* or *prt6-1* protoplasts confirmed that the $^{\Delta}$NOI2-HA and $^{\Delta}$NOI5-HA fragments were not N-degron pathway substrates. Interestingly, though, when the GFP-NOI3-HA fusion was coexpressed with AvrRpt2, the $^{\Delta}$NOI3-HA fragment was stabilized in a *prt6-1* mutant background, suggesting that it may be an N-degron substrate in Arabidopsis (Supplemental Fig. S9). No stabilization was observed in *ate1 ate2*, likely because of the lower expression levels of the proteins in this mutant background. Finally, coexpression of the double-tagged NOI1, NOI6, and NOI11 proteins with either HA-tagged AvrRpt2 or AvrRpt2^{H208A} indicated that in the presence of AvrRpt2, but not AvrRpt2^{H208A}, the $^{\Delta}$NOI-HA fragments were unstable in the Col-0 background. In contrast, the $^{\Delta}$NOI1-HA, $^{\Delta}$NOI6-HA, and $^{\Delta}$NOI11-HA fragments were stabilized in the *ate1 ate2* and *prt6-1* mutant backgrounds (Fig. 7). This stabilization confirms that the $^{\Delta}$NOI-HA fragments generated after cleavage of NOI1, NOI6, and NOI11 by AvrRpt2 are genuine N-degron pathway substrates in Arabidopsis.

DISCUSSION

Is the N-degron Pathway Involved in the Degradation of the RIN4-II and RIN4-III Fragments Generated after AvrRpt2 Proteolytic Cleavage?

Cleavage of RIN4 by the effector protease AvrRpt2 plays a key role in the onset of RPS2-mediated ETI. Several lines of evidence indicate that RIN4 fragments generated following AvrRpt2 cleavage are unstable (Axtell et al., 2003; Axtell and Staskawicz, 2003; Mackey et al., 2003), although several hours may be needed for their clearance (Kim et al., 2005a; Afzal et al., 2011). Importantly, the RIN4-II and -III fragments that are released after AvrRpt2 cleavage bear Asn or Asp, respectively, at their N termini (Chisholm et al., 2005), both of which are destabilizing N-terminal residues (Graciet et al., 2010). Here, we used antibodies raised against RIN4 (Liu et al., 2009) to determine if the N-degron pathway could be responsible for the degradation of the native RIN4-II and RIN4-III fragments that are released upon cleavage by AvrRpt2. We combined different approaches, including (1) the expression of mutated versions of RIN4 in which the newly exposed N-terminal residues were changed to stabilizing ones, (2) the monitoring of the RIN4-II and -III fragments released after cleavage of the endogenous RIN4 protein in wild-type and N-degron mutant backgrounds, and (3) the use of the recently developed tFT technique in plants (Zhang et al., 2019). The results of these experiments suggest that the RIN4-II and -III fragments are degraded within a few hours of AvrRpt2 expression in Col-0 AvrRpt2^{dex} lines or in *N. benthamiana*. However, contrary to what would be predicted if the fragments were N-degron substrates, the RIN4-II and -III fragments did not accumulate to detectable levels in *ate1 ate2* mutant plants that lack

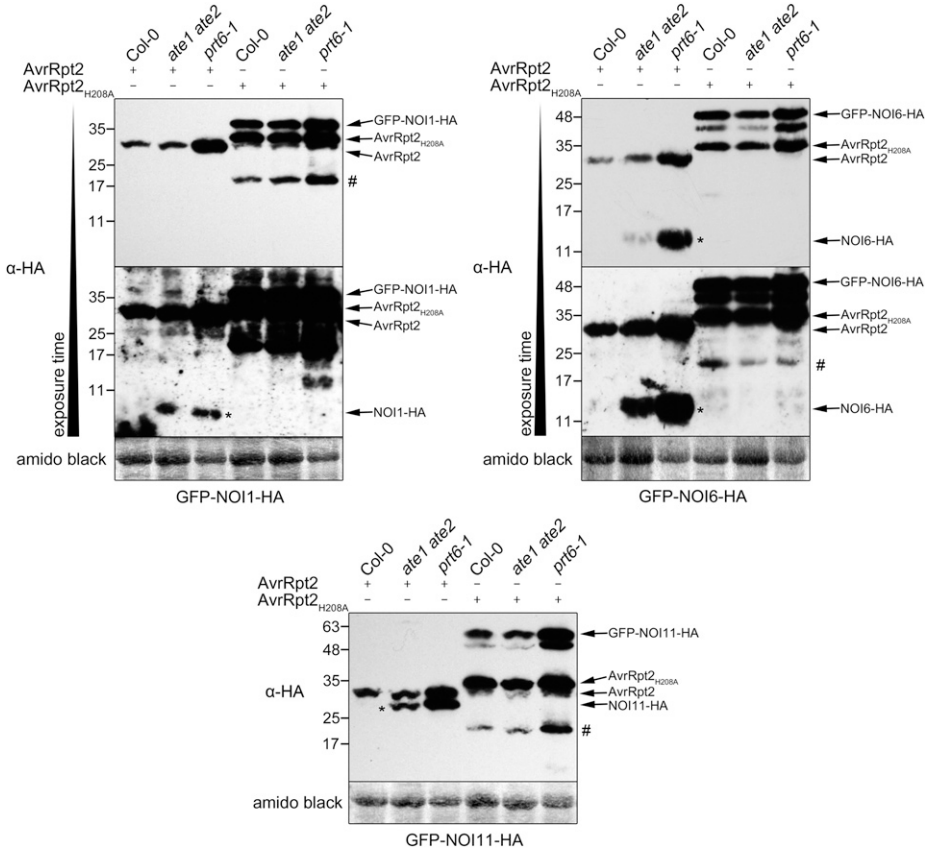

Figure 7. $^{\Delta}$NOI1-HA, $^{\Delta}$NOI6-HA, and $^{\Delta}$NOI11-HA fragments are stabilized in *ate1 ate2* and *prt6-1* mutant protoplasts. To address the stability of wild-type $^{\Delta}$NOI-HA fragments, protoplasts of wild-type Col-0 plants as well as *ate1 ate2* and *prt6-1* mutant plants were cotransfected with plasmids coding for the GFP-NOI-HA fusion proteins (NOI1, NOI6, and NOI11) and with plasmids encoding AvrRpt2-HA or AvrRpt2^{H208A}-HA. $^{\Delta}$NOI-HA C-terminal fragments (indicated with an asterisk) were detected using anti-HA antibodies (α-HA). Images of the same membrane with increasing exposure times are presented to show more clearly the stabilization of the different $^{\Delta}$NOI-HA fragments. #, Aspecific band. For all panels, original data are presented in Supplemental Figure S10. Data are representative of three independent replicates.

Arg-transferase activity (Graciet et al., 2009). Furthermore, mutation of the two newly exposed destabilizing N-termini (Asn-11 and Asp-153) into the stabilizing residue Gly was not sufficient to stabilize the RIN4-II and -III fragments after cleavage of $RIN4^{N11G}$ or $RIN4^{D153G}$ by AvrRpt2 in wild-type Arabidopsis or *N. benthamiana* plants. Altogether, our data suggest that a destabilizing N-terminal residue, such as Asn or Asp, is not necessary or sufficient for the degradation of the RIN4-II and -III fragments, respectively.

To more accurately compare the relative stability of the RIN4-II and -III fragments, we generated tFT constructs (Zhang et al., 2019) that allowed the expression of RIN4-II-tFT and RIN4-III-tFT fusion proteins through the ubiquitin fusion technique (Varshavsky, 2005) instead of AvrRpt2 cleavage. The stability of the resulting tFT constructs (which are designed to bear N-terminal Asn or Asp, respectively) was examined in wild-type Col-0 and *ate1 ate2* mutant plants, and no differences in the relative stabilities of each of the fragments were found. The results of these experiments hence provide additional support for the idea that the N-degron pathway may not be required for the instability of the two fragments. Surprisingly though, RIN4-II-tFT and RIN4-III-tFT did not exhibit the predicted cytosolic and plasma membrane localization, respectively (Kim et al., 2005a; Takemoto and Jones, 2005; Afzal et al., 2011). The tFT alone has a nucleocytoplasmic localization (Zhang et al., 2019), so that the punctuated localization of the RIN4-II-tFT and RIN4-III-tFT proteins is determined by the RIN4-II and -III fragments. In the case of the RIN4-III-tFT fusion protein, it is possible that the presence of the C-terminal tFT tag may have affected the palmitoylation of the three C-terminal Cys residues of RIN4 (Fig. 1A), hence also preventing the plasma membrane tethering of RIN4-III-tFT. However, it is unclear why the tFT fusion might have affected the cytosolic localization of the RIN4-II fragment, and whether this would have impaired the potential N-degron–mediated degradation of the fragments.

In summary, the data obtained in planta with full-length untagged RIN4 proteins strongly suggest that in plants in which RPS2 is functional, the native RIN4-II and RIN4-III fragments released after AvrRpt2 cleavage are not degraded by the N-degron pathway. Nevertheless, our data do not preclude a model whereby the RIN4-II and -III fragments could be degraded through the recognition of a combination of N-terminal and internal degrons, as has been suggested for RAP2.12, an N-degron pathway substrate that is also likely a substrate of the E3 ubiquitin ligase SEVEN IN ABSENTIA of Arabidopsis thaliana2 (Papdi et al., 2015). In the case of RIN4, the presence of an internal degron could still allow clearance of the RIN4 fragments in the absence of a destabilizing N-terminal residue (Fig. 8A). Yet another possibility suggested by the cellular localization of the RIN4-II-tFT and RIN4-III-tFT fusion proteins is that the two RIN4 fragments may be degraded via autophagy (Fig. 8A).

N-degron–Mediated Degradation of NOI Proteins

Identification of the consensus sequence recognized and cleaved by AvrRpt2 in substrate proteins led to identification of putative AvrRpt2 substrates (Chisholm et al., 2005) belonging to the family of NOI proteins (Afzal et al., 2013). Subsequently, these NOI proteins were shown to be cleaved by AvrRpt2 (with the exception of NOI10; Chisholm et al., 2005; Takemoto and Jones, 2005; Eschen-Lippold et al., 2016a). Notably, AvrRpt2 cleavage of several NOI proteins should result in protein fragments with a newly exposed destabilizing N-terminal residue (Table 1; Chisholm et al., 2005; Takemoto and Jones, 2005). Based on their phylogenetic relationship (Eschen-Lippold et al., 2016a), we selected a set of six NOI proteins (NOI1, NOI2, NOI3, NOI5, NOI6, and NOI11) and tested (1) the stability of the C-terminal fragments released by AvrRpt2 cleavage, and (2) the potential N-degron–mediated degradation of these fragments. Our experiments in *N. benthamiana* and wild-type Arabidopsis protoplasts with double-tagged, full-length NOI proteins (GFP-NOI-HA) indicate that the C-terminal fragments do not accumulate after cleavage by AvrRpt2. Introduction of point mutations to change the newly exposed N-terminal destabilizing residues into Ala, a stabilizing residue, was sufficient to stabilize the C-terminal fragments of NOI1, NOI6, and NOI11. Further comparison of the stability of the wild-type HA-tagged NOI C-terminal fragments in wild-type and in mutant *ate1 ate2* protoplasts following cleavage of the GFP-NOI-HA fusion proteins by AvrRpt2 confirmed that NOI1/6/11 constitute a set of N-degron substrates in plants. In addition, it is possible that the C-terminal fragment of NOI3 is also degraded by the N-degron pathway. The discovery of this set of N-degron substrates considerably expands the number of plant proteins that are targeted for degradation by the N-degron pathway. Thus far, the only known substrates of this pathway in plants were a set of group VII Ethylene Response Factors (ERF) transcription factors that act as master regulators of hypoxia response genes (Gibbs et al., 2011; Licausi et al., 2011), VERNALIZATION2 (Gibbs et al., 2018), as well as BIG BROTHER (Dong et al., 2017) and the more recently discovered LITTLE ZIPPER2 (Weits et al., 2019).

The physiological relevance of the N-degron–mediated degradation of these NOI fragments now needs to be explored in the context of the different and varied functions of AvrRpt2, including its roles in virulence and in the onset of RPS2-mediated ETI. Considering the sequence similarities between the NOI domain of these proteins and the C-terminal NOI domain of RIN4, it is possible that some of these fragments play a role in processes that are also regulated by RIN4, such as, for example, the repression of PTI. In this case, clearance of the C-terminal fragments by the N-degron pathway could provide a mechanism to alleviate the virulence-promoting activity of AvrRpt2 cleavage (Fig. 8B). Alternatively, cleavage of the NOI proteins could play a

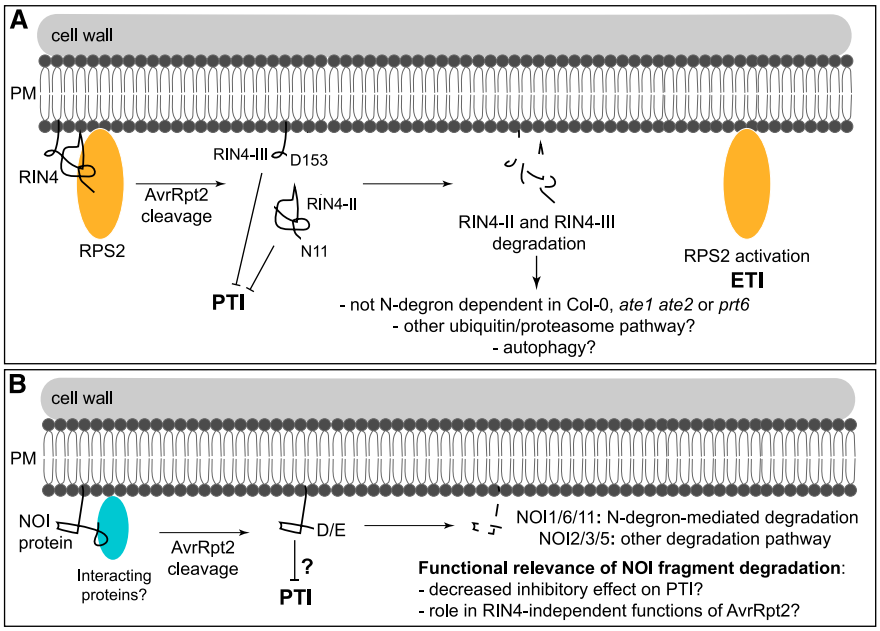

Figure 8. Proposed models and hypotheses for the degradation of RIN4 and NOI protein fragments generated after AvrRpt2 cleavage. A, RIN4 cleavage by AvrRpt2 releases two fragments with newly exposed N-terminal destabilizing residues (RIN4-II and RIN4-III). These fragments have been shown to suppress PTI in an *rpm1 rps2* mutant background (Afzal et al., 2011). In the presence of RPS2, RIN4 cleavage by AvrRpt2 triggers ETI. The fate of the RIN4-II and RIN4-III fragments suggests that they are targeted for degradation via an N-degron–independent mechanism possibly involving internal degron recognition by another ubiquitin/proteasome-dependent pathway or via autophagy. B, NOI domain proteins are also cleaved by AvrRpt2, and the resulting C-terminal fragments that start with N-terminal destabilizing residues are also unstable. Fragments of NOI1, NOI6, and NOI11 are N-degron pathway substrates, while fragments originating from NOI2/3/5 may be degraded through another pathway. The function of the NOI protein fragments obtained after AvrRpt2 cleavage remains to be explored. Similar to RIN4 fragments, they may play a role in the suppression of PTI or, alternatively, in mediating RIN4-independent functions of AvrRpt2. PM, Plasma membrane.

role in RIN4-independent functions of AvrRpt2, such as the repression of the flg22-induced activation of MAP KINASE4 and 11, the regulation of RPS2 signaling, or also in auxin-dependent mechanisms of AvrRpt2-induced virulence. Interestingly, not all NOIs may be cleaved by orthologs of AvrRpt2 encoded in the genomes of other bacteria, including some that are plant-associated rather than pathogenic (Eschen-Lippold et al., 2016a). Hence, it would also be interesting to study the role of the N-degron–mediated degradation of these NOI fragments in the context of the AvrRpt2 natural diversity.

Determinants of N-degrons in Plants

It is thought that most N-degron pathway substrates are generated through proteolytic cleavage (Rao et al., 2001; Varshavsky, 2011; Piatkov et al., 2012; Dissmeyer et al., 2018). However, our results highlight the fact that knowledge of proteolytic cleavage sites and of the identity of the newly exposed N-terminal residue is insufficient to accurately predict N-degron–mediated degradation. Classically, there are three determinants associated with an N-degron (Bachmair and Varshavsky, 1989; Varshavsky, 2011): (1) a destabilizing residue at the N terminus of the polypeptide chain, (2) a Lys residue for ubiquitin conjugation, and (3) sufficient flexibility of the polypeptide chain around the N terminus or near the ubiquitylation site. The RIN4-II and -III fragments as well as the different NOI fragments generated after AvrRpt2 cleavage all have the required attributes of an N-degron substrate in that they bear a newly exposed N-terminal destabilizing residue after AvrRpt2 cleavage, several Lys residues are present in the C-terminal domains, and all fragments are thought to be intrinsically unstructured (Sun et al., 2014; Lee et al., 2015a). Despite having these common attributes, only some of the fragments are N-degron pathway substrates. One possibility is that enzymatic components of the N-degron pathway may discriminate between these substrates based on the properties of the N-terminal region of the polypeptide chains. For example, the residue in the second position is known to influence the affinity or activity of both Arg-transferases and N-recognins toward their substrates (Choi et al., 2010; Matta-Camacho et al., 2010; Varshavsky, 2011; Wadas et al., 2016; Wang et al., 2018). While the exact effect of the amino acid residues neighboring the N terminus on Arg-transferase and PRT6 specificity in plants are not known, the conservation of the first two residues (Asp or Glu, followed by Trp) in all fragments released after

AvrRpt2 cleavage makes it unlikely to be the main determinant for selective degradation via the N-degron pathway. In addition, in the case of the RIN4-II fragment, whose 12-mer Asp-WEAEENVPYTA peptide that mimics the result of Asn-11 deamidation by NTAN1 could be arginylated in vitro, it is also possible that the specificity of NTAN1 may preclude recognition of the newly exposed Asn-11, although spontaneous deamidation of Asn-initiated proteins to Asp was seen previously (Wang et al., 2009). Alternatively, the observed peptide arginylation may be the result of the in vitro approach, which further highlights the need to test substrate degradation in planta.

Notably, similar observations were made for the family of group VII ERF transcription factors. In particular, some of these ERF transcription factors in rice—namely, ERF66, ERF67, and SUBMERGENCE1A-1 (SUB1A-1)—all have the attributes of an N-degron, as well as a conserved N-terminal region. Despite these common features, SUB1A-1 is not targeted for degradation by the N-degron pathway, while ERF66/67 are degraded via this pathway (Lin et al., 2019). The use of truncated proteins, as well as interaction assays, indicated that the C-terminal domain of SUB1A-1 could fold back onto the N-terminal region, thus precluding recognition of the N-terminal destabilizing residue by N-degron components (Lin et al., 2019). Interestingly, the N-terminal region of SUB1A-1 is also largely unstructured (Lin et al., 2019), similar to the RIN4 fragments and, presumably, the NOI fragments. Hence, it is possible that differences in the conformation of the different fragments released after AvrRpt2 cleavage could explain the different degradation mechanisms. Alternatively, protein-protein interactions between the different NOI domains and other proteins may also prevent N-degron degradation, depending on the interacting partner or the subcellular localization. The identification of protein interactors for both NOI domain proteins and RIN4 already suggests protein-specific interactomes for each of these AvrRpt2 substrates (Liu et al., 2009; Afzal et al., 2013), which may correlate with differential recognition by N-degron components.

MATERIALS AND METHODS

In Vitro Arginylation Assays

The synthesized RIN4 and RAP2 peptides had the X-WEAEENVPYTA or X-GGAIISDFIPP sequence, respectively, and each peptide included a C-terminal polyethylene glycol–biotin linker. For the arginylation assay, 1 μL of the purified His-ATE1 (corresponding to 0.5 μg of His-ATE1; cloning, expression, and purification of His-ATE1 are described in the Supplemental Materials) was incubated overnight at 30°C with 50 μL of the reaction mix (50 mM HEPES, pH 7.5; 25 mM KCl; 15 mM $MgCl_2$; 100 mM dithiothreitol; 2.5 mM ATP; 0.6 mg/mL *Escherichia coli* tRNA [Sigma-Aldrich]; 0.04 μg/μL *E. coli* aminoacyl-tRNA synthetase [Sigma-Aldrich]; 0.2 μCi ^{14}C-Arg) and 50 μM indicated peptide substrates. The next day, for each reaction, 50 μL of avidin agarose bead slurry (Thermo Scientific) was equilibrated in phosphate-buffered saline (PBS; 100 mM NaH_2PO_4, 150 mM NaCl, 0.2% [v/v] Nonidet P-40, pH 7.2) and resuspended in 350 μL of PBS. The reaction mixtures were added separately to 50 μL of avidin agarose bead and incubated at room temperature for 2 h with rotation. Subsequently, the beads were washed four times with 800 μL of PBS. Finally, the beads were resuspended in 1 mL of a scintillation solution. Scintillation counting was performed in a total of 4 mL of solution.

Plant Growth Conditions

Nicotiana benthamiana plants were grown on a medium consisting of compost, perlite, and vermiculite in a ratio of 5:2:3. The plants were grown under constant illumination at 20°C after being incubated at 4°C in the dark for 5 d.

Treatment of Plants with Dexamethasone

Col-0 AvrRpt2^{dex} Arabidopsis (*Arabidopsis thaliana*) seeds were grown in 3 mL of liquid 0.5× MS medium (2.2 g/L MS salts, pH 5.7) for 7 or 8 d with shaking at ~130 rpm in continuous light. Dexamethasone (Sigma-Aldrich), prepared as a stock solution of 10 mM in ethanol, was added to the growth medium to a final concentration of 10 μM. Whole seedlings were collected 5 h after the addition of dexamethasone to the medium. For each sample, 20–30 seedlings were pooled.

Pst AvrRpt2 and *Pst* AvrRpt2^{C122A} Inoculations of Wild-Type Col-0 and of *ate1 ate2* Mutant Plants for Immunoblot Analysis

Pst inoculations were performed on plants grown in Jiffy pots with a 9-h light period and a light intensity of 190 μmol/(m^2·s). *Pst* AvrRpt2 and *Pst* AvrRpt2^{C122A} were grown at 28°C on King's B medium supplemented with 6 mM $MgSO_4$. *Pst* strains were inoculated on 4-week-old plants following a high-humidity treatment 12 h before inoculation. A bacterial suspension at 5×10^7 colony forming units/mL in 10 mM $MgCl_2$ was infiltrated using a blunt syringe into the abaxial side of three leaves per plant. Three leaf discs (7 mm in diameter) from three different plants were collected at 8 hpi and pooled.

Generation of RIN4 Fragment Tandem Fluorescent Timers and GFP-NOI-HA or GFP-NOI^{mt}-HA–Coding Constructs

All cloning procedures are described in the Supplemental Materials. Oligonucleotides used and plasmids generated are listed in Supplemental Tables S1 and S2, respectively.

tFT Experiments

Transient expression experiments with the RIN4-II-tFT and RIN4-III-tFT constructs were carried out using 5-week-old Arabidopsis plants (Col-0 and *ate1 ate2*) using the protocol described by Mangano et al. (2014). For immunoblotting, leaf samples were harvested 4 d after transient transformation. Total leaf proteins were extracted in 50 mM HEPES-KOH, pH 7.8; 100 mM KCl; 5 mM EDTA; 5 mM EGTA; 1 mM NaF; 10% (v/v) glycerol; 1% (v/v) IGEPAL CA-630; 0.5% (w/v) sodium deoxycholate; 0.1% (w/v) SDS; 1 mM Na_4VO_3; 1 mM phenylmethylsulfonyl fluoride; and protease inhibitor cocktail (Roche). Samples were centrifuged for 15 min at 14,000*g*. Supernatant was mixed with 5× Laemmli buffer and boiled for 10 min at 95°C. Anti-GFP (clones 7.1 and 13.1; Roche) antibody was diluted 1:1,500 with Tris-buffered saline plus Tween 20 supplemented with 0.5% (v/v) western-blocking reagent (Roche). Confocal imaging was also conducted 4 d after agroinfiltration. Arabidopsis leaves were covered with water and analyzed using the A1 confocal laser-scanning microscope (Nikon). The fluorescence signal was imaged at 525/50 nm after excitation at 488 nm for sfGFP, and at 595/50 nm after excitation at 561 nm for mCherry. False color ratiometric images were generated after applying a Gaussian blur with a sigma of 1 and background subtraction in ImageJ (version 1.52h; https://imagej.nih.gov/ij). To quantify the mCherry to sfGFP ratio on a pixel-by-pixel basis, signal intensities of mCherry were divided by the intensities of the sfGFP using the image calculator of ImageJ. mCherry to sfGFP ratios were visualized by using the ImageJ lookup table "Fire." Since the mCherry to sfGFP ratio is sensitive to any microscopic setting, only ratios generated with identical configurations were compared.

Coexpression of RIN4 Constructs with AvrRpt2 and AvrRpt2^{C122A}

Coexpression of RIN4 constructs with AvrRpt2-FLAG or AvrRpt2^{C122A}-FLAG was carried out in a similar manner as previously described in Day et al. (2005). *Agrobacterium* strain C58 pGV2260 cells were transformed with the pMD-1 plasmids encoding the different RIN4 variants, AvrRpt2-FLAG, or AvrRpt2^{C122A}-FLAG and grown on LB (Luria-Bertani) agar with 50 mg/L rifampicin, 25 mg/L kanamycin, and 100 mg/L ampicillin for 3 d. After overnight growth in liquid culture with antibiotic selection, cells were collected by centrifugation and resuspended in infiltration medium (10 mM MES, pH 5.6; 10 mM $MgCl_2$; 150 μM acetosyringone) to a final OD_{600} of 0.4 (RIN4 variants) and 0.1 (AvrRpt2-FLAG or AvrRpt2^{C122A}-FLAG). The *Agrobacterium* suspensions were syringe infiltrated into the abaxial side of *N. benthamiana* leaves (two leaves per plant; two plants per condition). Four half leaves collected from four leaves of the two infiltrated plants were pooled at 24 h, followed by freezing in liquid nitrogen and protein extraction.

Transient Gene Expression in *N. benthamiana* Followed by Inoculation of *Pseudomonas syringae*

Agrobacterium strain C58 pGV2260 cells were transformed with binary pMD-1 plasmids encoding RIN4 variants or with pML-BART plasmids encoding GFP-NOI-HA constructs and grown on LB agar with 50 mg/L rifampicin, 100 mg/L spectinomycin, and 100 mg/L ampicillin for 3 d. After overnight growth in liquid culture with 100 mg/L spectinomycin and 100 mg/L ampicillin, cells were collected by centrifugation and resuspended in infiltration medium (10 mM MES, pH 5.6; 10 mM $MgCl_2$; 150 μM acetosyringone) to a final OD_{600} of 0.75. The *Agrobacterium* suspensions were syringe infiltrated into the abaxial side of *N. benthamiana* leaves (two leaves per plant; two plants per condition).

P. syringae pathovar tomato DC3000 carrying a plasmid encoding AvrRpt2, AvrRpt2^{C122A}, or an empty plasmid was streaked onto an LB agar plate with 25 mg/L kanamycin, 5 mg/L tetracyclin, and 100 mg/L rifampicin and grown for 2 d at 28°C. Cells from these plates were then resuspended in 10 mM $MgCl_2$ to an OD_{600} of 0.7 before being infiltrated into previously agroinfiltrated *N. benthamiana* leaves using a 1-mL syringe. *Pst* infiltration was performed 72 h after the initial agroinfiltration. For each sample, four half leaves collected from four leaves of the two infiltrated plants were pooled at 24 h, followed by freezing in liquid nitrogen and protein extraction.

Protein Extraction and Immunoblotting

To prepare total protein extracts from plant tissue (Arabidopsis or *N. benthamiana*) for immunoblotting, plant tissue was ground to a fine powder in liquid nitrogen. This powder was then resuspended in 2× SDS loading buffer. Samples were spun at 18,000*g* for 10 min, and supernatant was transferred to a new 1.5-mL tube. This step was repeated before samples were placed at 95°C for 5 min. Samples were centrifuged at 18,000*g* for 10 min, and supernatant was used for subsequent analysis.

Primary antibodies used in this study for immunoblotting were anti-GFP (1:5,000; Abcam #Ab290), anti-HA (1:1,000; Sigma #H3663), anti-RIN4#1 (1:2,000; Mackey et al., 2002), antiRIN4#2 (1:2,000; Liu et al., 2009), and anti-RIN4#3 (aN-13, 1:200; Santa Cruz #sc-27369). Secondary antibodies used were anti-rabbit horseradish peroxidase (HRP; A0545, Sigma-Aldrich) and anti-mouse HRP (A9044, Sigma-Aldrich), both diluted 1:50,000. All antibodies were prepared in PBS plus Tween 20 supplemented with 5% (w/v) milk powder.

Plant Growth Conditions and Transient Expression in Protoplasts

Arabidopsis wild type (Col-0), *prt6-1*, and the double mutant *ate1 ate2* were grown on soil in a climate chamber for 5 to 6 weeks under controlled conditions (22°C, 8-h light/16-h darkness; 140 μE). Isolation and transfection of protoplasts were performed as described by Yoo et al. (2007). Protoplasts coexpressing AvrRpt2 (wild type/H208A) and double-tagged NOI proteins (N-terminal GFP, C-terminal HA) were harvested by centrifugation after 16-h incubation at 18°C in the dark. Protoplast pellets were mixed with standard SDS-loading buffer, boiled for 5 min (95°C), and total protein samples were used for SDS-PAGE and immunoblotting. All antibodies were diluted in 1× Tris-buffered saline plus Tween 20 with 3% (w/v) milk powder (primary antibodies: anti-GFP JL-8 [1:5,000], Takara Bio #632381; anti-HA.11 16B12 [1:1,000], Biozol #BLD-901515; secondary antibody: anti-mouse HRP [1:10,000], Sigma-Aldrich #A9044).

Confocal Imaging to Visualize GFP-NOI-HA Protein Subcellular Localization

Agrobacterium strain C58 pGV2260 cells were transformed with pML-BART vector encoding the different GFP-NOI-HA constructs and grown on LB agar with antibiotic selection for 3 d. After overnight growth in liquid culture with antibiotic selection, cells were collected by centrifugation and resuspended in infiltration medium (10 mM MES, pH 5.6; 10 mM $MgCl_2$; 150 μM acetosyringone) to a final OD_{600} of 0.75. Cells were syringe infiltrated into the abaxial side of *N. benthamiana* leaves. Three days after agroinfiltration, an Olympus FluoView1000 laser-scanning confocal microscope was used to visualize GFP fluorescence from the abaxial leaf side. For control (untreated) samples, a small leaf section was cut and deposited abaxial side down into water for confocal imaging. For plasmolysis experiments, the same leaf section was transferred abaxial side down into a 1-M NaCl solution. Confocal imaging was carried out immediately in the salt solution. A 488-nm excitation wavelength was used. GFP signal was collected at 500–550 nm, and autofluorescence signal was collected at 600–700 nm. All imaging conditions were kept constant for all experiments.

Accession numbers

Sequence data from this article can be found in The Arabidopsis Information Resource (TAIR) database under accession numbers At3g25070 (RIN4), At5g63270 (NOI1), At5g40645 (NOI2), At2g17660 (NOI3), At5g64850 (NOI6), At3g07195 (NOI11). Please also refer to accession numbers in the legend to Figure 1, as well as in Table 1.

Supplemental Data

The following supplemental materials are available.

Supplemental Figure S1. Alignment of AvrRpt2 cleavage sites in RIN4 from monocots.

Supplemental Figure S2. Uncropped immunoblots shown in Figure 2.

Supplemental Figure S3. Immunoblots shown in Figure 3.

Supplemental Figure S4. Representative false-color images of cells transiently expressing N-RIN4-II-tFT in wild-type or in *ate1 ate2* plants.

Supplemental Figure S5. Representative false-color images of cells transiently expressing D-RIN4-III-tFT in wild-type or in *ate1 ate2* plants.

Supplemental Figure S6. Subcellular localization of GFP-NOI-HA proteins.

Supplemental Figure S7. Uncropped immunoblots shown in Figure 5.

Supplemental Figure S8. Uncropped immunoblots shown in Figure 6.

Supplemental Figure S9. $^{\Delta}$NOI2-HA, $^{\Delta}$NOI3-HA, and $^{\Delta}$NOI5-HA fragment stability in *ate1 ate2* and *prt6-1* mutant protoplasts.

Supplemental Figure S10. Uncropped immunoblots shown in Figure 7.

Supplemental Table S1. List of oligonucleotides used.

Supplemental Table S2. List of plasmids generated for this study.

Supplemental Materials. Supplementary methods and materials.

ACKNOWLEDGMENTS

We are very grateful to Stephen Chisholm and Brian Staskawicz for sharing the pMD-1 RIN4, pMD-1 RIN4^{N11G}, and pMD-1 RIN4^{D153G} plasmids; the *Pst* AvrRpt2 and *Pst* AvrRpt2^{C122A} strains; as well as the *rps2 rin4*, Col-0 AvrRpt2-^{dex} lines, and the anti-RIN4#1 antiserum. We thank Gitta Coaker for sharing the purified RIN4-specific antibody (anti-RIN4#2), as well as the pMD-1 plasmids coding for AvrRpt2-FLAG or AvrRpt2^{C122A}-FLAG. We also thank Dr. Ilona Dix

for help with confocal imaging, Nicole Bauer for excellent technical assistance, and Brian Mooney for comments on the manuscript. We also thank Prof. Alexander Varshavsky for helpful discussions and initial support for the work.

Received February 28, 2019; accepted June 13, 2019; published June 21, 2019.

LITERATURE CITED

Abbas M, Berckhan S, Rooney DJ, Gibbs DJ, Vicente Conde J, Sousa Correia C, Bassel GW, Marín-de la Rosa N, León J, Alabadí D, et al (2015) Oxygen sensing coordinates photomorphogenesis to facilitate seedling survival. Curr Biol **25:** 1483–1488

Afzal AJ, da Cunha L, Mackey D (2011) Separable fragments and membrane tethering of *Arabidopsis* RIN4 regulate its suppression of PAMP-triggered immunity. Plant Cell **23:** 3798–3811

Afzal AJ, Kim JH, Mackey D (2013) The role of NOI-domain containing proteins in plant immune signaling. BMC Genomics **14:** 327

Axtell MJ, Staskawicz BJ (2003) Initiation of RPS2-specified disease resistance in Arabidopsis is coupled to the AvrRpt2-directed elimination of RIN4. Cell **112:** 369–377

Axtell MJ, Chisholm ST, Dahlbeck D, Staskawicz BJ (2003) Genetic and molecular evidence that the Pseudomonas syringae type III effector protein AvrRpt2 is a cysteine protease. Mol Microbiol **49:** 1537–1546

Bachmair A, Varshavsky A (1989) The degradation signal in a short-lived protein. Cell **56:** 1019–1032

Chen Z, Agnew JL, Cohen JD, He P, Shan L, Sheen J, Kunkel BN (2007) *Pseudomonas syringae* type III effector AvrRpt2 alters *Arabidopsis thaliana* auxin physiology. Proc Natl Acad Sci USA **104:** 20131–20136

Chisholm ST, Dahlbeck D, Krishnamurthy N, Day B, Sjolander K, Staskawicz BJ (2005) Molecular characterization of proteolytic cleavage sites of the *Pseudomonas syringae* effector AvrRpt2. Proc Natl Acad Sci USA **102:** 2087–2092

Choi WS, Jeong BC, Joo YJ, Lee MR, Kim J, Eck MJ, Song HK (2010) Structural basis for the recognition of N-end rule substrates by the UBR box of ubiquitin ligases. Nat Struct Mol Biol **17:** 1175–1181

Coaker G, Falick A, Staskawicz B (2005) Activation of a phytopathogenic bacterial effector protein by a eukaryotic cyclophilin. Science **308:** 548–550

Couto D, Zipfel C (2016) Regulation of pattern recognition receptor signalling in plants. Nat Rev Immunol **16:** 537–552

Cui F, Wu S, Sun W, Coaker G, Kunkel B, He P, Shan L (2013) The *Pseudomonas syringae* type III effector AvrRpt2 promotes pathogen virulence via stimulating Arabidopsis auxin/indole acetic acid protein turnover. Plant Physiol **162:** 1018–1029

Day B, Dahlbeck D, Huang J, Chisholm ST, Li D, Staskawicz BJ (2005) Molecular basis for the RIN4 negative regulation of RPS2 disease resistance. Plant Cell **17:** 1292–1305

de Marchi R, Sorel M, Mooney B, Fudal I, Goslin K, Kwaśniewska K, Ryan PT, Pfalz M, Kroymann J, Pollmann S, et al (2016) The N-end rule pathway regulates pathogen responses in plants. Sci Rep **6:** 26020

Desveaux D, Singer AU, Wu AJ, McNulty BC, Musselwhite L, Nimchuk Z, Sondek J, Dangl JL (2007) Type III effector activation via nucleotide binding, phosphorylation, and host target interaction. PLoS Pathog **3:** e48

Dissmeyer N (2019) Conditional protein function via N-degron pathway-mediated proteostasis in stress physiology. Annu Rev Plant Biol **70:** 83–117

Dissmeyer N, Rivas S, Graciet E (2018) Life and death of proteins after protease cleavage: Protein degradation by the N-end rule pathway. New Phytol **218:** 929–935

Dong H, Dumenil J, Lu FH, Na L, Vanhaeren H, Naumann C, Klecker M, Prior R, Smith C, McKenzie N, (2017) Ubiquitylation activates a peptidase that promotes cleavage and destabilization of its activating E3 ligases and diverse growth regulatory proteins to limit cell proliferation in *Arabidopsis*. Genes Dev **31:** 197–208

Eschen-Lippold L, Jiang X, Elmore JM, Mackey D, Shan L, Coaker G, Scheel D, Lee J (2016a) Bacterial AvrRpt2-like cysteine proteases block activation of the arabidopsis mitogen-activated protein kinases, MPK4 and MPK11. Plant Physiol **171:** 2223–2238

Eschen-Lippold L, Scheel D, Lee J (2016b) Teaching an old dog new tricks: Suppressing activation of specific mitogen-activated kinases as a potential virulence function of the bacterial AvrRpt2 effector protein. Plant Signal Behav **11:** e1257456

Garzón M, Eifler K, Faust A, Scheel H, Hofmann K, Koncz C, Yephremov A, Bachmair A (2007) *PRT6*/At5g02310 encodes an *Arabidopsis* ubiquitin ligase of the N-end rule pathway with arginine specificity and is not the *CER3* locus. FEBS Lett **581:** 3189–3196

Gibbs DJ, Lee SC, Isa NM, Gramuglia S, Fukao T, Bassel GW, Correia CS, Corbineau F, Theodoulou FL, Bailey-Serres J, et al (2011) Homeostatic response to hypoxia is regulated by the N-end rule pathway in plants. Nature **479:** 415–418

Gibbs DJ, Bacardit J, Bachmair A, Holdsworth MJ (2014) The eukaryotic N-end rule pathway: Conserved mechanisms and diverse functions. Trends Cell Biol **24:** 603–611

Gibbs DJ, Bailey M, Tedds HM, Holdsworth MJ (2016) From start to finish: Amino-terminal protein modifications as degradation signals in plants. New Phytol **211:** 1188–1194

Gibbs DJ, Tedds HM, Labandera AM, Bailey M, White MD, Hartman S, Sprigg C, Mogg SL, Osborne R, Dambire C, et al (2018) Oxygen-dependent proteolysis regulates the stability of angiosperm polycomb repressive complex 2 subunit VERNALIZATION 2. Nat Commun **9:** 5438

Graciet E, Wellmer F (2010) The plant N-end rule pathway: Structure and functions. Trends Plant Sci **15:** 447–453

Graciet E, Walter F, Ó'Maoiléidigh DS, Pollmann S, Meyerowitz EM, Varshavsky A, Wellmer F (2009) The N-end rule pathway controls multiple functions during *Arabidopsis* shoot and leaf development. Proc Natl Acad Sci USA **106:** 13618–13623

Graciet E, Mesiti F, Wellmer F (2010) Structure and evolutionary conservation of the plant N-end rule pathway. Plant J **61:** 741–751

Gravot A, Richard G, Lime T, Lemarié S, Jubault M, Lariagon C, Lemoine J, Vicente J, Robert-Seilaniantz A, Holdsworth MJ, et al (2016) Hypoxia response in *Arabidopsis* roots infected by *Plasmodiophora brassicae* supports the development of clubroot. BMC Plant Biol **16:** 251

Henry E, Yadeta KA, Coaker G (2013) Recognition of bacterial plant pathogens: Local, systemic and transgenerational immunity. New Phytol **199:** 908–915

Holman TJ, Jones PD, Russell L, Medhurst A, Ubeda Tomás S, Talloji P, Marquez J, Schmuths H, Tung SA, Taylor I, et al (2009) The N-end rule pathway promotes seed germination and establishment through removal of ABA sensitivity in *Arabidopsis*. Proc Natl Acad Sci USA **106:** 4549–4554

Jin P, Wood MD, Wu Y, Xie Z, Katagiri F (2003) Cleavage of the *Pseudomonas syringae* type III effector AvrRpt2 requires a host factor(s) common among eukaryotes and is important for AvrRpt2 localization in the host cell. Plant Physiol **133:** 1072–1082

Jones JD, Dangl JL (2006) The plant immune system. Nature **444:** 323–329

Khmelinskii A, Keller PJ, Bartosik A, Meurer M, Barry JD, Mardin BR, Kaufmann A, Trautmann S, Wachsmuth M, Pereira G, et al (2012) Tandem fluorescent protein timers for in vivo analysis of protein dynamics. Nat Biotechnol **30:** 708–714

Khmelinskii A, Meurer M, Ho CT, Besenbeck B, Füller J, Lemberg MK, Bukau B, Mogk A, Knop M (2016) Incomplete proteasomal degradation of green fluorescent proteins in the context of tandem fluorescent protein timers. Mol Biol Cell **27:** 360–370

Kim HS, Desveaux D, Singer AU, Patel P, Sondek J, Dangl JL (2005a) The *Pseudomonas syringae* effector AvrRpt2 cleaves its C-terminally acylated target, RIN4, from *Arabidopsis* membranes to block RPM1 activation. Proc Natl Acad Sci USA **102:** 6496–6501

Kim MG, da Cunha L, McFall AJ, Belkhadir Y, DebRoy S, Dangl JL, Mackey D (2005b) Two Pseudomonas syringae type III effectors inhibit RIN4-regulated basal defense in Arabidopsis. Cell **121:** 749–759

Kourelis J, van der Hoorn RAL (2018) Defended to the nines: 25 years of resistance gene cloning identifies nine mechanisms for R protein function. Plant Cell **30:** 285–299

Kulich I, Pečenková T, Sekereš J, Smetana O, Fendrych M, Foissner I, Höftberger M, Zárský V (2013) Arabidopsis exocyst subcomplex containing subunit EXO70B1 is involved in autophagy-related transport to the vacuole. Traffic **14:** 1155–1165

Lee D, Bourdais G, Yu G, Robatzek S, Coaker G (2015a) Phosphorylation of the plant immune regulator RPM1-INTERACTING PROTEIN4 enhances plant plasma membrane H^+-ATPase activity and inhibits flagellin-triggered immune responses in Arabidopsis. Plant Cell **27:** 2042–2056

Lee J, Manning AJ, Wolfgeher D, Jelenska J, Cavanaugh KA, Xu H, Fernandez SM, Michelmore RW, Kron SJ, Greenberg JT (2015b) Acetylation of an NB-LRR plant immune-effector complex suppresses immunity. Cell Reports **13:** 1670–1682

Licausi F, Kosmacz M, Weits DA, Giuntoli B, Giorgi FM, Voesenek LA, Perata P, van Dongen JT (2011) Oxygen sensing in plants is mediated by an N-end rule pathway for protein destabilization. Nature **479:** 419–422

Lin CC, Chao YT, Chen WC, Ho HY, Chou MY, Li YR, Wu YL, Yang HA, Hsieh H, Lin CS, et al (2019) Regulatory cascade involving transcriptional and N-end rule pathways in rice under submergence. Proc Natl Acad Sci USA **116:** 3300–3309

Liu J, Elmore JM, Fuglsang AT, Palmgren MG, Staskawicz BJ, Coaker G (2009) RIN4 functions with plasma membrane H+-ATPases to regulate stomatal apertures during pathogen attack. PLoS Biol **7:** e1000139

Liu N, Hake K, Wang W, Zhao T, Romeis T, Tang D (2017) CALCIUM-DEPENDENT PROTEIN KINASE5 associates with the truncated NLR protein TIR-NBS2 to contribute to exo70B1-mediated immunity. Plant Cell **29:** 746–759

Mackey D, Holt III BF, Wiig A, Dangl JL (2002) RIN4 interacts with Pseudomonas syringae type III effector molecules and is required for RPM1-mediated resistance in Arabidopsis. Cell **108:** 743–754

Mackey D, Belkhadir Y, Alonso JM, Ecker JR, Dangl JL (2003) Arabidopsis RIN4 is a target of the type III virulence effector AvrRpt2 and modulates RPS2-mediated resistance. Cell **112:** 379–389

Mangano S, Gonzalez CD, Petruccelli S (2014) *Agrobacterium tumefaciens*-mediated transient transformation of *Arabidopsis thaliana* leaves. Methods Mol Biol **1062:** 165–173

Matta-Camacho E, Kozlov G, Li FF, Gehring K (2010) Structural basis of substrate recognition and specificity in the N-end rule pathway. Nat Struct Mol Biol **17:** 1182–1187

Mendiondo GM, Gibbs DJ, Szurman-Zubrzycka M, Korn A, Marquez J, Szarejko I, Maluszynski M, King J, Axcell B, Smart K, et al (2016) Enhanced waterlogging tolerance in barley by manipulation of expression of the N-end rule pathway E3 ligase PROTEOLYSIS6. Plant Biotechnol J **14:** 40–50

Papdi C, Pérez-Salamó I, Joseph MP, Giuntoli B, Bögre L, Koncz C, Szabados L (2015) The low oxygen, oxidative and osmotic stress responses synergistically act through the ethylene response factor VII genes RAP2.12, RAP2.2 and RAP2.3. Plant J **82:** 772–784

Piatkov KI, Brower CS, Varshavsky A (2012) The N-end rule pathway counteracts cell death by destroying proapoptotic protein fragments. Proc Natl Acad Sci USA **109:** E1839–E1847

Potuschak T, Stary S, Schlögelhofer P, Becker F, Nejinskaia V, Bachmair A (1998) *PRT1* of *Arabidopsis thaliana* encodes a component of the plant N-end rule pathway. Proc Natl Acad Sci USA **95:** 7904–7908

Rao H, Uhlmann F, Nasmyth K, Varshavsky A (2001) Degradation of a cohesin subunit by the N-end rule pathway is essential for chromosome stability. Nature **410:** 955–959

Sabol P, Kulich I, Žárský V (2017) RIN4 recruits the exocyst subunit EXO70B1 to the plasma membrane. J Exp Bot **68:** 3253–3265

Schuessele C, Hoernstein SN, Mueller SJ, Rodriguez-Franco M, Lorenz T, Lang D, Igloi GL, Reski R (2016) Spatio-temporal patterning of arginyl-tRNA protein transferase (ATE) contributes to gametophytic development in a moss. New Phytol **209:** 1014–1027

Stary S, Yin XJ, Potuschak T, Schlögelhofer P, Nizhynska V, Bachmair A (2003) PRT1 of Arabidopsis is a ubiquitin protein ligase of the plant N-end rule pathway with specificity for aromatic amino-terminal residues. Plant Physiol **133:** 1360–1366

Stegmann M, Anderson RG, Westphal L, Rosahl S, McDowell JM, Trujillo M (2013) The exocyst subunit *Exo70B1* is involved in the immune response of *Arabidopsis thaliana* to different pathogens and cell death. Plant Signal Behav **8:** e27421

Sun X, Greenwood DR, Templeton MD, Libich DS, McGhie TK, Xue B, Yoon M, Cui W, Kirk CA, Jones WT, et al (2014) The intrinsically disordered structural platform of the plant defence hub protein RPM1-interacting protein 4 provides insights into its mode of action in the host-pathogen interface and evolution of the nitrate-induced domain protein family. FEBS J **281:** 3955–3979

Takemoto D, Jones DA (2005) Membrane release and destabilization of *Arabidopsis* RIN4 following cleavage by *Pseudomonas syringae* AvrRpt2. Mol Plant Microbe Interact **18:** 1258–1268

Toruño TY, Shen M, Coaker G, Mackey D (2019) Regulated disorder: Posttranslational modifications control the RIN4 plant immune signaling hub. Mol Plant Microbe Interact **32:** 56–64

van der Hoorn RAL, Kamoun S (2008) From guard to decoy: A new model for perception of plant pathogen effectors. Plant Cell **20:** 2009–2017

Varshavsky A (2005) Ubiquitin fusion technique and related methods. Methods Enzymol **399:** 777–799

Varshavsky A (2011) The N-end rule pathway and regulation by proteolysis. Protein Sci **20:** 1298–1345

Varshavsky A (2019) N-degron and C-degron pathways of protein degradation. Proc Natl Acad Sci USA **116:** 358–366

Vicente J, Mendiondo GM, Movahedi M, Peirats-Llobet M, Juan YT, Shen YY, Dambire C, Smart K, Rodriguez PL, Charng YY, et al (2017) The Cys-Arg/N-end rule pathway is a general sensor of abiotic stress in flowering plants. Curr Biol **27:** 3183–3190

Vicente J, Mendiondo GM, Pauwels J, Pastor V, Izquierdo Y, Naumann C, Movahedi M, Rooney D, Gibbs DJ, Smart K, et al (2019) Distinct branches of the N-end rule pathway modulate the plant immune response. New Phytol **221:** 988–1000

Wadas B, Piatkov KI, Brower CS, Varshavsky A (2016) Analyzing N-terminal arginylation through the use of peptide arrays and degradation assays. J Biol Chem **291:** 20976–20992

Wang H, Piatkov KI, Brower CS, Varshavsky A (2009) Glutamine-specific N-terminal amidase, a component of the N-end rule pathway. Mol Cell **34:** 686–695

Wang J, Pejaver VR, Dann GP, Wolf MY, Kellis M, Huang Y, Garcia BA, Radivojac P, Kashina A (2018) Target site specificity and in vivo complexity of the mammalian arginylome. Sci Rep **8:** 16177

Weits DA, Kunkowska AB, Kamps NCW, Portz KMS, Packbier NK, Nemec Venza Z, Gaillochet C, Lohmann JU, Pedersen O, van Dongen JT, et al (2019) An apical hypoxic niche sets the pace of shoot meristem activity. Nature **569:** 714–717

White MD, Klecker M, Hopkinson RJ, Weits DA, Mueller C, Naumann C, O'Neill R, Wickens J, Yang J, Brooks-Bartlett JC, et al (2017) Plant cysteine oxidases are dioxygenases that directly enable arginyl transferase-catalysed arginylation of N-end rule targets. Nat Commun **8:** 14690

Wilton M, Subramaniam R, Elmore J, Felsensteiner C, Coaker G, Desveaux D (2010) The type III effector $HopF2_{Pto}$ targets *Arabidopsis* RIN4 protein to promote *Pseudomonas syringae* virulence. Proc Natl Acad Sci USA **107:** 2349–2354

Yoo SD, Cho YH, Sheen J (2007) Arabidopsis mesophyll protoplasts: A versatile cell system for transient gene expression analysis. Nat Protoc **2:** 1565–1572

Zhang H, Gannon L, Hassall KL, Deery MJ, Gibbs DJ, Holdsworth MJ, van der Hoorn RAL, Lilley KS, Theodoulou FL (2018) N-terminomics reveals control of Arabidopsis seed storage proteins and proteases by the Arg/N-end rule pathway. New Phytol **218:** 1106–1126

Zhang H, Linster E, Gannon L, Leemhuis W, Rundle CA, Theodoulou FL, Wirtz M (2019) Tandem fluorescent protein timers for non-invasive relative protein lifetime measurement in plants. Plant Physiol **180:** 718–731